

Synthesis and Characterization of Polyacrylamide and *Poly(acrylamide-co-diallyldimethylammonium chloride)* via Free-Radical and RAFT Polymerization

by  
Hannah Welch

A thesis presented to the Honors College of Middle Tennessee State  
University in partial fulfillment of the requirements for graduation from  
the University Honors College

Term Spring 2021

Thesis Committee:

Dr. Dwight Patterson

Dr. Kevin Bicker, Second Reader

Dr. Gregory Van Patten, Thesis Committee Chair

Synthesis and Characterization of Polyacrylamide and Poly(acrylamide-co-diallyldimethylammonium chloride) via Free-Radical and RAFT Polymerization

by  
Hannah Welch

APPROVED:

---

Dr. Dwight Patterson, Thesis Director  
Professor, Department of Chemistry

---

Dr. Gregory Van Patten, Thesis Committee Chair  
Chair, Department of Chemistry

## ACKNOWLEDGEMENTS

I owe much appreciation and respect to my thesis advisor, Dr. Dwight Patterson, for guiding me through this research project. He provided an infinite supply of knowledge and encouragement along the way, and I admire his continuous passion for polymers. I would also like to thank my momma for the support and steady optimism, and the love of science pursuits that I inherited from her. Finally, I want to thank Robbie Mahaffey for keeping me laughing and sharing in the triumphs and defeats, the epic highs and lows of scientific research with me. A special shoutout to Donut Country and the local Starbucks for never failing to provide sustenance, energy, and hope throughout this project.

## ABSTRACT

First synthesized decades ago, acrylamide-based polymers have blossomed into one of the most important polymers in the modern-day era. The uses of polyacrylamides are plentiful and varied, from their main application in waste-water treatment to paper making processes. The water solubility and large molecular weights of these polymers make them extremely useful for coagulation methods as well. Acrylamide itself reacts easily with a wide array of polyelectrolytes, expanding the function possibilities even more. Free-radical synthesis has been a vital mode of creation in previous years, but in more recent times, new and improved synthesis methods have been discovered. RAFT polymerization in particular is well-known for its ease of use and for its ability to maximize polymer content control. This research focuses on the synthesis and characterization of these acrylamide-based polymers with an intent to deepen an understanding of their polymeric properties. To do this, compounds were synthesized using acrylamide and diallyldimethylammonium chloride. Both free-radical and RAFT polymerization methods were used as well. The products were characterized using nuclear magnetic resonance, Fourier transform infrared spectroscopy, and dilute-solution viscosity tests. Thermal properties were obtained using thermogravimetric analysis and differential scanning calorimetry. The hypothesized product structures were proven correct with analysis methods. RAFT and free-radical synthesis were compared, but more in-depth research is required to isolate the differences in molecular compositions.

## TABLE OF CONTENTS

LIST OF TABLES.....	vii
LIST OF FIGURES.....	viii
CHAPTER I: INTRODUCTION.....	1
A. Background.....	1
B. Polymerization Syntheses.....	2
1. Free Radical Polymerization.....	3
2. RAFT Synthesis.....	7
C. Purpose of this Study.....	11
CHAPTER II: MATERIALS AND METHODS.....	13
A. General Experiment Details.....	13
B. Synthesis.....	14
1. Free-Radical Synthesis of Polyacrylamide.....	14
2. Free Radical Synthesis of Poly(acrylamide-co-diallyldimethylammonium- chloride).....	16
3. RAFT Synthesis of Polyacrylamide through Microwave Synthesis.....	18
C. Analysis Methods.....	22
1. Thermogravimetric Analysis.....	22
2. DSC Analysis.....	22
3. Fourier Transform Infrared (FTIR) Spectroscopy.....	22
4. NMR Analysis.....	23
5. Dilute Solution Viscosity Analysis.....	23

CHAPTER III: RESULTS AND DISCUSSIONS.....	25
A. FTIR.....	25
B. NMR.....	34
C. Thermogravimetric Analysis.....	45
D. Differential Scanning Calorimetry.....	48
E. Dilute Solution Viscosity.....	51
CHAPTER IV: CONCLUSIONS.....	54
REFERENCES.....	55
APPENDIX.....	58
A. NMR Spectroscopy Data.....	58
B. Thermal Analysis Data.....	62
C. FTIR Analysis Data.....	63

## LIST OF TABLES

TABLE	PAGE
1. Compositions of A-Series polyacrylamide samples, showing grams of initiator and acrylamide, with product yield, theoretical yield, and percent yield.....	15
2. Compositions of E-Series samples, showing grams of initiator and co-monomers, with product yield, theoretical yield, and percent yield.....	17
3. Compositions of G-Series polyacrylamide samples, showing grams of RAFT agent, initiator, and acrylamide, with product yield, theoretical yield, and percent yield..	19
4. Viscosity tests solution concentrations and time measurements of A5 sample.....	24
5. Viscosity tests solution concentrations and calculations based off time measurements of sample A5.....	24
6. Peak Assignments for A3, E8, and G4 samples with corresponding functional groups.....	33
7. <sup>1</sup> H NMR Peak Assignments of Samples A8, E4, and G4.....	34
8. Comparison of Tacticities between <sup>13</sup> C NMR Samples A8 and G4.....	45
9. Degradation Onsets of Series A, E, and G.....	45
10. T <sub>g</sub> , T <sub>m</sub> , and Heat of Fusion for Series A, E, and G.....	48
11. Intrinsic Viscosities and Molecular weights of A Series.....	53

## LIST OF FIGURES

FIGURE	PAGE
1. Process of acrylamide-based polymer interacting with a particle suspension to form large flocs.....	2
2. Examples of diverse ways in which copolymers can be manipulated using controlled/living polymerizations.....	3
3. General mechanism of initiator radicalizing in response to heat.....	4
4. Molecular structure of 4,4'-Azobis(4-cyanopentanoic acid).....	4
5. Molecular structure of 4,4'-Azobis(4-cyanopentanoic acid) radical.....	5
6. a. Molecular structure of acrylamide monomer.....	5
b. Molecular structure of polyacrylamide.....	5
7. Example of propagation of acrylamide monomers into a chain polymer.....	6
8. a. Molecular structure of diallyldimethylammonium chloride.....	7
b. Molecular structure of co-polymer poly(acrylamide-co diallyldimethylammonium chloride).....	7
9. A comparison of the chain lengths of tradition free-radical polymerization and RAFT polymerization.....	8
10. Flow chart of causalities of a suitable RAFT agent and a well-defined polymer.....	9
11. Structure of RAFT agent 2-cyano-2-propyl benzodithioate.....	9
12. Mechanism of RAFT polymerization with legend.....	11
13. Energy and Temperature plots of G-Series Microwave synthesis.....	20
14. Parameters of microwave synthesis polymerization for G Series.....	21
15. FTIR overlay plots of A Series.....	26
16. FTIR overlay plots of E Series.....	27

17. FTIR overlay plots of G Series.....	28
18. FTIR stack plots of A Series, E Series and G Series .....	29
19. : FTIR stack plots of A Series, E Series, and G Series.(2380-3850cm <sup>-1</sup> ).....	30
20. FTIR stack plots of A Series, E Series, and G Series (550-1900cm <sup>-1</sup> ).....	31
21. FTIR plots Sample A3 specific peak assignments.....	32
22. <sup>13</sup> C NMR (D <sub>2</sub> O) Sample A8.....	35
23. . <sup>1</sup> H NMR (D <sub>2</sub> O) Sample A8.....	36
24. . <sup>13</sup> C NMR (D <sub>2</sub> O) Sample E4.....	37
25. <sup>1</sup> H NMR (D <sub>2</sub> O) Sample E4.....	38
26. <sup>13</sup> C NMR (D <sub>2</sub> O) Sample G4.....	39
27. . <sup>1</sup> H NMR (D <sub>2</sub> O) Sample G4.....	40
28. Zoomed-In <sup>13</sup> C NMR (D <sub>2</sub> O) Sample A8.....	43
29. Zoomed-In <sup>13</sup> C NMR (D <sub>2</sub> O) Sample G4.....	44
30. Overlay Plot of TGA thermogram for A Series.....	47
31. Overlay Plot of DSC thermogram for A, E and G Series.....	50
32. Legend for Huggins and Kraemer Plot for calculating Intrinsic Viscosity.....	51
33. Huggins/Kraemer overlay graphs of Sample A9.....	51
34. Huggins/Kraemer overlay graphs of Sample E4.....	52
35. Huggins/Kraemer overlay graphs of Sample G4.....	52

## CHAPTER I: INTRODUCTION

### A. Background

Water-soluble polymers have been the objects of intrigue and subsequent research for many years due to their vast array of uses. The last couple decades have seen an explosion in uses for acrylamide-based polymers particularly.<sup>1-3</sup> Acrylamide is an advantageous monomer because it can be modified in different ways to create linear copolymers with an array of cationic, anionic, and non-ionic monomers, each with different functionalities. The extremely high molecular weight of polymers also has a variety of applications. Because of this, acrylamides and their polymer derivatives are used in waste-water treatment as flocculants, in petroleum industries, paper-making industries, and agricultural settings.<sup>4</sup> In fact, the market for polyacrylamide has become so expansive in recent years that it is expected to hit a value of \$6.68 billion by the year 2023.<sup>4</sup>

A cationic monomer commonly paired with acrylamide is diallyldimethylammonium chloride, or DADMAC. DADMAC was first discovered to be profitable in the 1940s, when initially diallyldimethylammonium bromide was synthesized and radically cyclopolymerized to form a polymer, then converted to its chloride form<sup>5</sup>. Because of its cationic nature, it was highly soluble in water.<sup>6</sup> Diallyldimethylammonium chloride has more recently been paired with acrylamide monomers in the 1980s to create a high molecular weight polymer used mainly for flocculation.<sup>7,8</sup> This polymer is called Poly(acrylamide-co-diallyldimethylammonium chloride). Polymeric flocculants are most sought after because they require smaller doses, cost cheaper, and settle impurities out of

solutions much more effectively than other flocculating agents.<sup>9</sup> **Figure 1** below shows the process by which a polyacrylamide flocculant can coagulate with impurities in water.

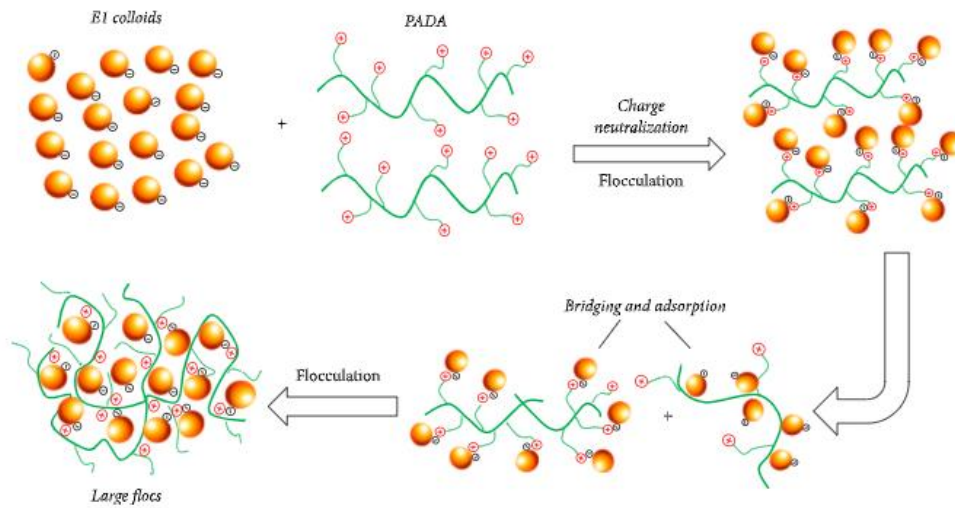


**Figure 1.** Process of acrylamide-based polymers interacting with a particle suspension to form large flocs.<sup>10</sup> From “Synthesis of a Cationic Polyacrylamide under UV Initiation and Its Flocculation in Estrone Removal”, by Jiaoxia Sun et al., 2018, *International Journal of Polymer Science*, 2018, p.9. Published with Creative Commons Attribution License.

Due to the massive importance of polymers in today’s global industry and scientific research, specifically polyacrylamide and poly(acrylamide-co-diallyldimethylammonium chloride), this study is devoted to obtaining a deeper knowledge of both the synthesis and characterization of these polymers.

## B. Polymerization Syntheses

Two different kinds of polymerization, free radical and controlled radical, will be evaluated in this study. Free radical polymerization is a simple process in which vinyl monomers (molecules containing carbon-carbon double bonds) react in the presence of a

catalyst and are polymerized randomly in a solution.<sup>11</sup> The monomer levels and uniformity of the polymer chain cannot be controlled. However, newer methods have been developed that make it possible to control the polymerization process so that monomer layout can be sculpted as desired, and the resulting polymer molecules are uniform. This is known as CRP, controlled radical polymerization.<sup>12</sup> Various techniques such as stable free radical mediated polymerization, atom transfer radical polymerization (ATRP), and reversible addition-fragmentation chain transfer (RAFT) are all subtypes of controlled radical polymerization.<sup>13</sup> **Figure 2.** illustrates these benefits.

## What Can Controlled/ Living Polymerizations Do ?

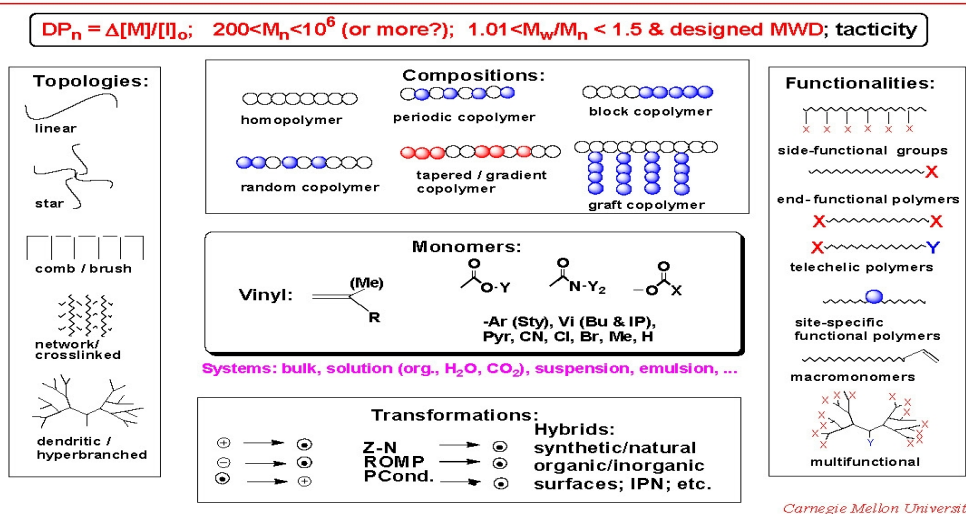


**Figure 2.** Examples of diverse ways in which copolymers can be manipulated using controlled/living polymerizations.<sup>14</sup> From Features of Controlled "Living" Radical polymerizations - Matyjaszewski polymer group - Carnegie Mellon University. <https://www.cmu.edu/maty/crp/features.html>. Copyright 2001 by Carnegie Mellon. Reprinted with permission.

### 1. Free Radical Polymerization

Free radical polymerization is a specific type of chain-growth polymerization, which is the process of creating a chain of molecules through a reactive intermediate.

There are several reactions possible, such as radical polymerization, cationic polymerization, and anionic polymerization. The reactions depend on what initiators are used and what monomers. In this study, an acid, 4,4'-Azobis(4-cyanovaleric acid), or 4,4'-Azobis(4-cyanopentanoic acid), is used as a radical initiator. According to literature, 4,4'-Azobis(4-cyanovaleric acid) is commonly used in heterogenous and homogenous free-radical polymerizations involving polyvinyl chlorides, polyacrylonitriles, and polyvinyl alcohols.<sup>15</sup> To start the polymerization process, the initiator reacts in the presence of heat to form radicals, which then interact with the *in situ* monomers. The mechanism of the radical formation is shown below in **Figure 3**.

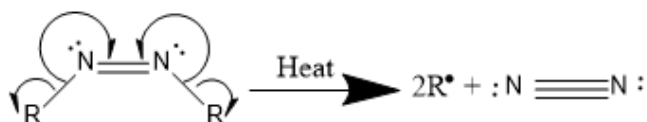


**Figure 3.** General mechanism of initiator radicalizing in response to heat.

In the presence of heat, the N-R bonds break, creating two radical groups and a triple bond between the nitrogen atoms. Those radical groups then react with a monomer to form a reactive monomer end group, which can lead to chain propagation. The structure of 4,4'-Azobis(4-cyanopentanoic acid) is shown in **Figure 4**.

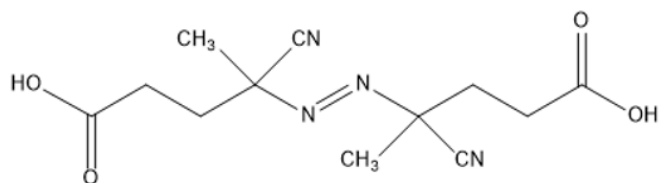


**Figure 4.** Molecular structure of 4,4'-Azobis(4-cyanopentanoic acid).

The sites of bond breakage are in between the two nitrogens and their adjacent carbons. and nitrogen-3 and carbon-4, as labelled in Figure 6, leaving a triple bond between N-2 and N-3, and two radical R groups. The resulting radical R group is shown in **Figure 5**.

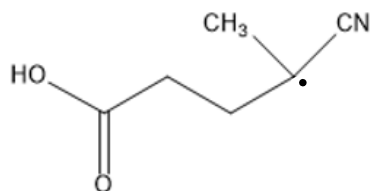
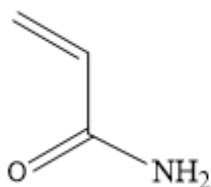
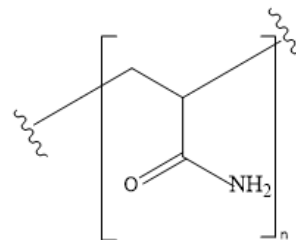


**Figure 5.** Molecular structure of 4,4'-Azobis(4-cyanopentanoic acid) radical.

When mixed in a solution with acrylamide, the initiator sets off an extensive reaction. The structure of acrylamide is shown in **Figure 6.a**, and **Figure 6.b** shows the molecular structure of acrylamide once it has been exposed to a radical and chain-linked with other monomers.



**a.**



**b.**

**Figure 6.a.** Molecular structure of acrylamide monomer.

**Figure 6.b.** Molecular structure of polyacrylamide.

When the acrylamide molecule is exposed to a radicalized initiator, the radical attacks the double bond between the alpha and beta carbons attaching onto the beta carbon. The alpha carbon is now left with an extra electron, becoming a radical itself. The new radical attacks another acrylamide monomer, elongating until, ideally, there are no more acrylamide monomers left in the solution. This process is shown in **Figure 7**.

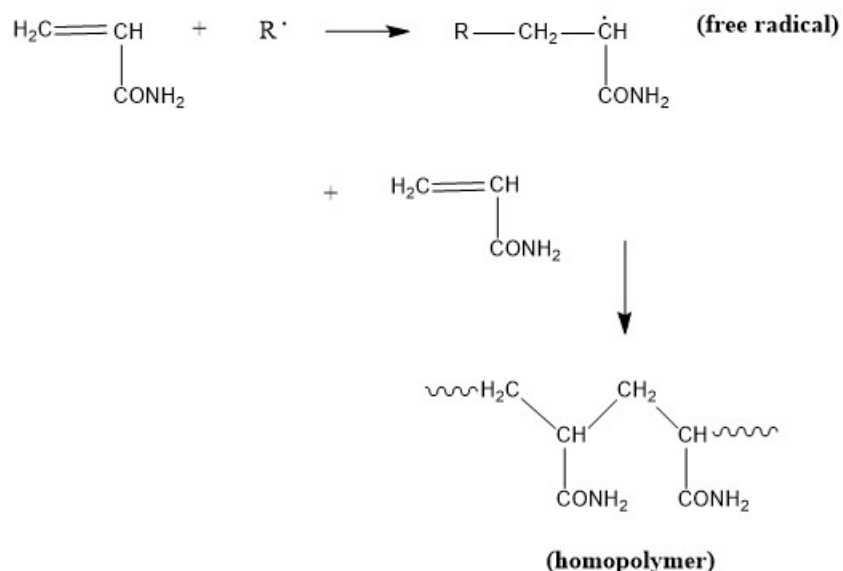


**Figure 7.** Example of propagation of acrylamide monomers into a chain polymer.<sup>16</sup>

This study involves the free-radical synthesis of both polyacrylamide and poly(acrylamide-co-diallyldimethylammonium chloride). The formation of polyacrylamide was previously discussed; a simple homo-polymer chain elongation. The free-radical polymerization of a heteropolymer involving two or more types of monomer, such as acrylamide and DADMAC, is a very similar process. **Figure 8.a** shows the molecular structure of DADMAC and **Figure 8.b** portrays the molecular structure of poly(acrylamide-co-diallyldimethylammonium chloride).

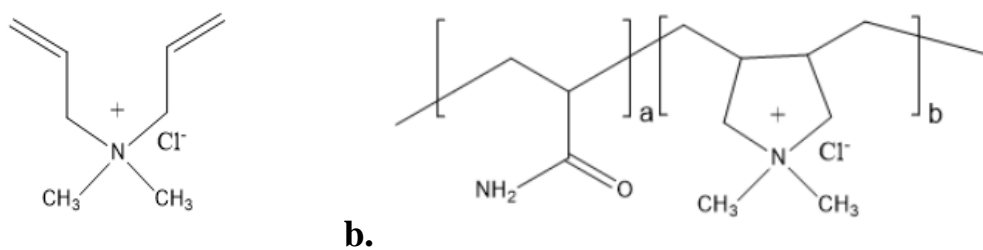


**Figure 8.a.** Molecular structure of diallyldimethylammonium chloride.

**Figure 8.b.** Molecular structure of co-polymer poly(acrylamide-co-diallyldimethylammonium chloride).

Co-polymerization DADMAC includes begins with an initiation step, with a radical attacking a C=C bond and opening it. Cyclization then occurs as the remaining C=C is broken open, which leaves an open radical waiting to react with another monomer. The result is a polymer with a backbone of cyclic units and extremely hydrophilic charged quaternary ammonium groups on each monomer.<sup>17</sup> This makes for a strong polyelectrolyte with a high molecular weight.<sup>18</sup> However, because the reaction is a free-radical polymerization, there is little control over the distribution or amount of the DADMAC interspersed throughout the acrylamide monomers.

## 2. RAFT Synthesis

The next synthesis performed was a form of controlled radical polymerization known as RAFT, or **R**eversible **A**ddition-**F**ragmentation chain-**T**ransfer. RAFT polymerization is useful for better control of molecular weight and low molecular weight distribution in comparison to free-radical polymerizations.<sup>19</sup> A visual of this is provided in **Figure 9**.

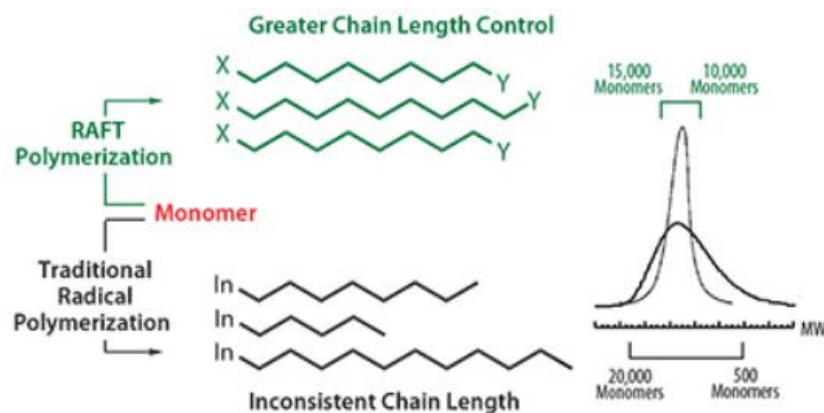


**Figure 9.** A comparison of the chain lengths of tradition free-radical polymerization and RAFT polymerization.<sup>22</sup> From Concepts and tools for raft polymerization. <https://www.sigmaaldrich.com/technical-documents/articles/crp-guide/concepts-and-tools-for-raft-polymerization.html>. Copyright Sigma-Aldrich, Inc. Reprinted with permission.

RAFT was first discovered in 1998 by Tam. P.Le, Graeme Moad, Ezio Rizzardo, and San H. Thang.<sup>20</sup> It can be used to polymerize a large variety of monomers, such as (meth)acrylates, acrylonitriles, and (meth)acrylamides.<sup>21</sup> Laboratory synthesis procedures for this form of polymerization are similar to free radical polymerization synthesis. The difference lies in adding a thiocarbonylthio compound into the reaction, which is known as a chain-transfer agent, or a RAFT agent. RAFT agents must be chosen carefully to properly react with the chosen monomers. For example, cyanomethyl diphenylcarbomodithioate is most suited for vinyl acetates and vinyl benzoates. The necessity for a compatible agent lies in the reaction kinetics of the polymerization, as well as the agent solubility.<sup>22</sup> A characteristic of a good raft agent is that its C=S bond is more reactive to radicals than the alkene of the co-monomers, which is dependent upon the Z- and R- groups of the RAFT agent.<sup>23</sup> This is supported by the flow chart in **Figure 10**. A RAFT agent must have a reactive C=S bond, an R group that is both a good leaving

group and can reinitiate polymerization, and a Z group that influences the reaction kinetics of radical addition and fragmentation.

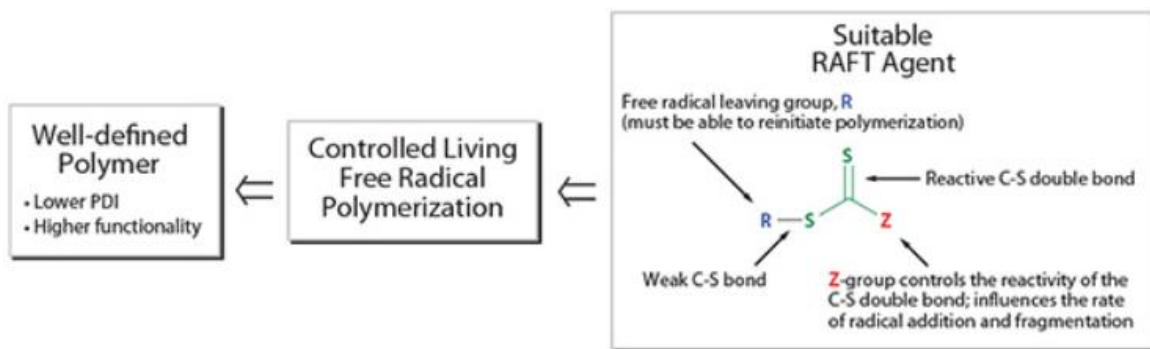


**Figure 10.** Flow chart of causalities of a suitable RAFT agent and a well-defined polymer.<sup>22</sup> From Concepts and tools for raft polymerization. <https://www.sigmaaldrich.com/technical-documents/articles/crp-guide/concepts-and-tools-for-raft-polymerization.html>. Copyright Sigma-Aldrich, Inc. Reprinted with permission.

The RAFT agent used in this study is 2-cyano-2-propyl benzodithioate, which is compatible with (meth)acrylate and (meth)acrylamide monomers.<sup>22</sup> The structure of 2-cyano-2-propyl benzodithioate is shown in **Figure 11**.

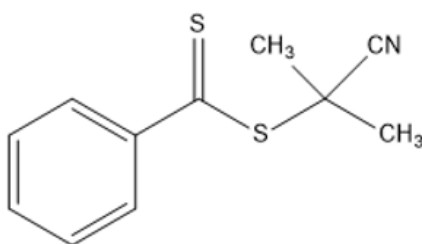
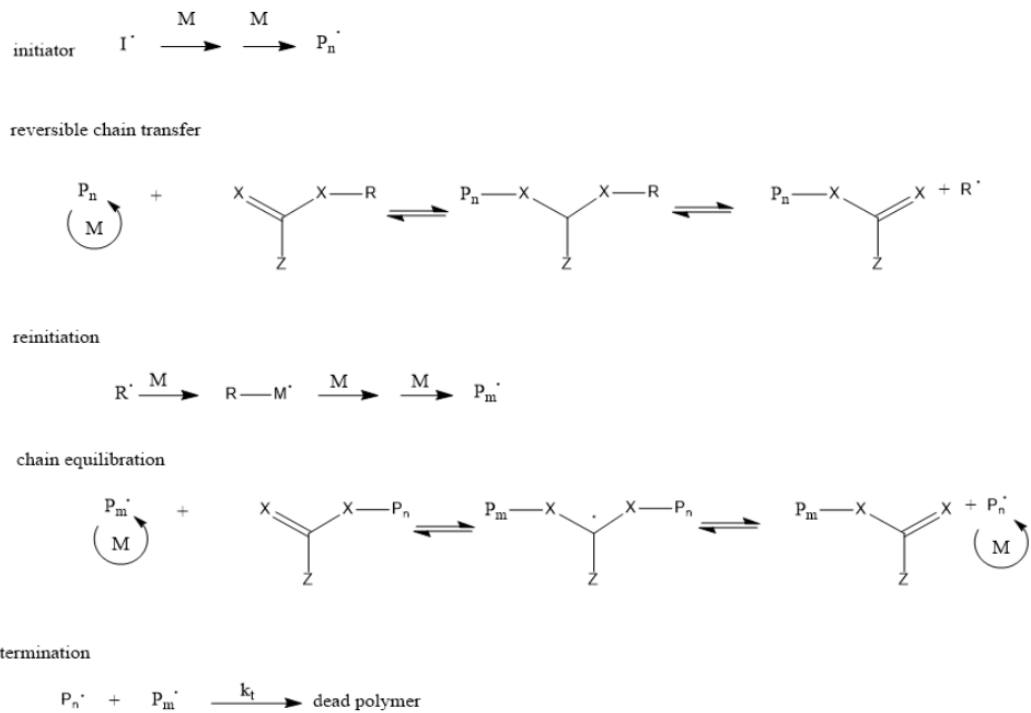


**Figure 11.** Structure of RAFT agent 2-cyano-2-propyl benzodithioate.

With an appropriate RAFT agent determined, the synthesis proceeds. This kind of CRP is dependent on an equilibrium between active and dormant chains.<sup>23</sup> A source of radicals is needed, which is provided by a radical initiator. In this study, the same radical

initiator is used for both CRP and free-living polymerization, which is 4,4'-Azobis(4-cyanopentanoic acid). The process begins with initiator radical activation through thermal decomposition, kicking off a small chain growth with the monomers. The RAFT agent then binds to the chain; its thiocarbonylthio group inhibiting the chain radicals and creating a new intermediate radical. This implements an equilibrium between the active and dormant chains in the solution.<sup>24</sup> The new intermediate will then fragment into an original radical species that reinitiates chain growth.<sup>24</sup> If the RAFT agent was chosen carefully, the forward reaction (creating an original group) will dominate, and the leaving group  $R^\bullet$  will be kicked off instead of the polymeric species. That  $R^\bullet$  leaving group then reacts with another monomer, in the process of re-initiation. Through this inhibit/initiate reversible system, the reaction reaches an equilibrium. The rate of addition/fragmentation should exceed the rate of propagation, resulting in chains that have similar DPs (degree of polymerization), which ultimately results in uniform polymers.<sup>25</sup> Termination occurs when two radicals react to form a dead polymer.<sup>26</sup> This entire process is portrayed in **Figure 12.** along with a legend explaining the symbol meanings.



RAFT Polymerization Mechanism Legend	
Symbol	Definition
$I^{\cdot}$	Initiator Radical
$M$	Monomers
$P_n^{\cdot}$	1 <sup>st</sup> Propagating Radical
$R^{\cdot}$	New Radical formed from intermediate radical
$P_m^{\cdot}$	New (2 <sup>nd</sup> ) Propagating Radical

**Figure 12.** Mechanism of RAFT polymerization with legend.

### C. Purpose of this Study

The primary goal of this work will be to further understand the complex processes of free-radical and RAFT polymerization through synthesis and characterization of polymer products. A homopolymer and a co-polymer will be created via free-radical polymerization using the monomer acrylamide (AM), and acrylamide and DADMAC, respectively. A homopolymer synthesized through controlled radical polymerization with acrylamide will also be created. The reaction will be carried out in aqueous solution, as it

is the most common and cheapest method. The resulting polymeric products will be studied using a variety of polymer characterization techniques, such as FTIR, NMR, TGA, DSC, and dilute-solution viscosity analysis. Through these analyses, the structure, molecular weight, and various properties will be assigned to the polymeric products.

## CHAPTER II: MATERIALS AND METHODS

This chapter provides in-depth descriptions of the synthesis procedures and materials used. First, free-radical polymerization of homopolymer polyacrylamide will be discussed. Free-radical polymerization of heteropolymer acrylamide-diallyldimethylammonium chloride will then be described. Finally, the process of controlled polymerization synthesis of both homogenous and PAM-co-DADMAC copolymers will be discussed.

### A. General Experiment Details

All solvents, reagents, and labware used were commercially available, without any purification or further processing. NMR data were attained using a 500 MHz FT-NMR model ECA-500 JEOL (Peabody, MA), bought by MTSU Chemistry Department. To dry the samples, the Isotemp Vacuum Oven Model 281A, (Fisher Scientific) was used. Thermal analysis was carried out using Differential Scanning Calorimetry instrument, model DSC Q2000, and Thermogravimetric Analysis instrument, model TGA Q500. Infrared data was obtained using the iS50 FTIR w/ ATR (Thermo Scientific) instrument. A Koehler Kinematic Viscosity Bath was used to measure the dilute -solution viscosity and behavior of the resulting polymeric systems.

## B. Synthesis

### 1. Free-Radical Synthesis of Polyacrylamide

Twelve samples, known as Series A, was the first series to be synthesized. First, a 1 M solution of acrylamide was created by adding dry, powdered acrylamide (7.105 g, 0.1 mol) to 100 mL of DI H<sub>2</sub>O. This was degassed for O<sub>2</sub> by passing argon gas for 15 minutes by inserting a pipette emitting gas into the solution and slowly stirring. It was kept in an air tight container, sealed with PM-992 Parafilm at 8°C. The initiator, 4,4'-Azobis(4-cyanopentanoic acid)(≥91.5%), was then measured out into twelve 20 mL cylinder vials. A1-A3 contained ~0.0280 g, 0.1 mmol of initiator, A4-A6 (~0.0560 g, 0.2 mmol), A7-A9 (~0.0840 g, 0.3 mmol) and A10-A12 (~0.1121 g, 0.4 mmol). Ten milliliters of the acrylamide solution were then pipetted into each vial, and solutions were purged for five minutes each with nitrogen gas. Vials were then placed on a Fine Vortex FINEPCR vibrator, stirring the mixtures for thirty seconds. However, as the solutions were being mixed, and indeed, as soon as the initiator came into contact with the solution, they started to polymerize, forming an opaque, jelly-like substance before they could be exposed to heat, which was troubling to say the least, as acrylamide is not supposed to polymerize at room temperature. The samples were then processed for analysis. This involved removing the polymerized gel from vials and placing into twelve 250 mL beakers with 200 mL of DI H<sub>2</sub>O. These were covered in parafilm and placed on 50 °C heating plate with stir bars for ~48 hours. When fully dissolved, beakers were removed from heat and placed into fridge for cooling. Precipitation methods were used to extract the pure product from the solution of DI H<sub>2</sub>O. Chilled liquid methanol (500 mL, ≥99.6%)

was poured separately into twelve 800 mL beakers to use as an anti-solvent. The polymer solution was then poured slowly into the methanol, while stirring vigorously with a glass rod to coagulate the precipitating polymers. Using methanol as a solvent proved to be only partly successful, as the solution became murky, and it was obvious only a fraction of the polymer was precipitating out of solution. The beakers were then placed in the fridge for a further 24 hours to gather more precipitation. After filtration, the samples were placed in glass petri dishes and dried in the vacuum oven for 38 hours at 50 °C. Once samples were dried, they were stored and then analyzed. The sample products were very firm pellets of material, neither flexible nor brittle. They were an opaque white in color. **Table 1** shows the polymer compositions of Series A.

**Table 1.** Compositions of A-Series polyacrylamide samples, showing grams of initiator and acrylamide, with product yield, theoretical yield, and percent yield.

Samples A1-A12:	4,4'-Azo-bis (4-cyano-valeric acid) (g):	Acrylamide (g):	Product (g):	Theoretical Yield (g):	Percent Yield (%)
A1	0.0281	0.7108	0.592	0.7389	80.1
A2	0.0280	0.7108	0.466	0.7388	63.1
A3	0.0280	0.7108	0.711	0.7388	96.2
A4	0.0560	0.7108	0.595	0.7668	77.6
A5	0.0561	0.7108	0.625	0.7669	81.5
A6	0.0561	0.7108	0.723	0.7669	94.3
A7	0.0838	0.7108	0.792	0.7946	99.7
A8	0.0840	0.7108	0.512	0.7948	64.4
A9	0.0838	0.7108	0.783	0.7946	98.5
A10	0.1120	0.7108	0.789	0.8228	95.9
A11	0.1121	0.7108	0.491	0.8229	59.7
A12	0.1120	0.7108	0.777	0.8228	94.4

Series B-D were then devoted to figuring out why the Series A solution polymerized immediately. Through this investigation it was eventually ascertained that a smaller amount of initiator was required. While Series A used ~ 0.0280-0.1120 grams of initiator (1% - 4% molar ratio of initiator to acrylamide), Series E-G used a substantially less amount. Series E had a 0.1% - 0.5% molar ratio and Series G contained a 0.5% molar

ratio of initiator to AM. Theoretically, larger amounts of initiator should not trigger a polymerization reaction. Without an exposure to heat, the initiator should not radicalize. Further research is required to pinpoint the cause of immediate polymerization.

## **2. Free Radical Synthesis of Poly(acrylamide-co-diallyldimethylammonium chloride)**

Upon discovering the issue with the initiator, the E series was created, adding another monomer into the mix. The added monomer was diallylmethylammonium chloride ( $\geq 97.0\%$ , (AT)), or DADMAC. There were 8 samples, 1E-8E, with varying levels of both DADMAC and initiator. 1E-2E were composed of  $\sim 0.0028$  g initiator, 0.0808 g (0.5 mmol) DADMAC; 3E-4E ( $\sim 0.0140$  g initiator, 0.161 g (1 mmol) DADMAC; 5E-6E ( $\sim 0.0140$  g initiator, 0.0808 g (0.5 mmol) DADMAC; 7E-8E ( $\sim 0.0028$  g initiator, 0.161 g (1 mmol) DADMAC. The samples were prepared in a comparable way to the A series. The anhydrous monomers were measured out and added to 10 mL of 1 M acrylamide solution, then stirred for 15 min with magnetic stir bars, until solutions were clear and colorless. The solutions were then purged with nitrogen for 5 minutes each, wrapped securely with foil (six layers), and placed on a 70 °C warming pad for 2 hours until polymerization. With the lower amount of initiator, the samples did not polymerize until exposed to heat, as expected from literature.<sup>27</sup> The precipitation process used in A series was repeated as well, using 200 mL of DI H<sub>2</sub>O and 50 °C to dissolve the eight separate polymer samples, which were cooled and then precipitated using methanol. The precipitations did not yield the desired results, even when stirring most vigorously and pouring slowly. The amount of solute that came out was very little, even when

beakers were left for a week to settle out. It was also hoped the methanol would evaporate, leaving the polymers behind. After seven days, roughly 100 mL of polymer/methanol solution was left. It was hypothesized that the solvent may not be the most efficient, and using acetone was then approached. The remaining amount of the solutions, which were foggy and had much unprecipitated polymer, were poured into separate beakers containing 600 mL of acetone. White, stringy solid material immediately precipitated, proving acetone to be a much more effective anti-solvent. The precipitate was then filtered out, placed in petri dishes, and dried in vacuum oven in the same way as A series, then stored for further evaluation. Immediately, it was apparent that the E series was much more brittle than A series, indicating straight away the compositions were different. **Table 2** below shows the compositions of samples E1-E8.

**Table 2.** Compositions of E-Series samples, showing grams of initiator and co-monomers, with product yield, theoretical yield, and percent yield.

Samples E1-E8:	4,4'-Azo-bis (4-cyano-valeric acid)	Acrylamide (g):	Diallyldimethyl-ammonium chloride (g):	Product (g):	Theoretical Yield (g):	Percent Yield (%)
<b>E1</b>	0.0025	0.7108	0.0803	0.592	0.7936	74.6
<b>E2</b>	0.0024	0.7108	0.0811	0.466	0.7943	58.7
<b>E3</b>	0.0143	0.7108	0.1619	0.711	0.8870	80.2
<b>E4</b>	0.0142	0.7108	0.1621	0.595	0.8871	67.1
<b>E5</b>	0.0139	0.7108	0.0806	0.625	0.8053	77.6
<b>E6</b>	0.0141	0.7108	0.0811	0.723	0.8060	89.7
<b>E7</b>	0.0030	0.7108	0.1619	0.792	0.8757	90.4
<b>E8</b>	0.0024	0.7108	0.1610	0.512	0.8742	58.6

### 3. RAFT Synthesis of Polyacrylamide through Microwave Synthesis

The preparation of polyacrylamide through RAFT synthesis involved reacting a RAFT agent 2-Cyano-2-propyl benzodithioate with initiator 4,4'-Azo-bis (4-cyano-valeric acid) and a solution of acrylamide. The new series was labelled as the **G Series** and will be referred to the G series from here on. The F Series involved a calculation error in the amount of grams of RAFT agent used, so further analysis and characterization was not acquired. The G Series procedure started with calculating the correct raft agent to initiator molar ratio. According to literature, several of the most effective ratios are  $[RAFT]/[I] = 1.67, 3.33, \text{ and } 6.67$ , respectively.<sup>22</sup> From series E, it was determined that 0.0140 grams of 4,4'-Azo-bis (4-cyano-valeric acid) provided the most consistent and highest yielding products, leading to that amount being used for each sample in the G series, and from that the RAFT agent amount was calculated. The anhydrous reagents were measured and mixed with 3 mL of 1 M acrylamide solution in a 4 mL screw-cap glass vial. The vials were purged with argon gas for 5 minutes each, then placed on 30 °C and stirred with a magnetic stir bar until the reagents were evenly distributed, roughly 15 minutes. The samples were then placed in the microwave to polymerize. Upon removal, the samples appeared only slightly viscous and pink in color, due to the RAFT agent. Precipitation of the samples involved slowly pouring the contents into a 50 mL beaker containing ~40 mL of acetone while stirring with a spatula. White polymers immediately formed, but there were still traces of polymer residues left in the acetone. The samples were centrifuged at 4000 rpm for 30 minutes to gather the polymers, which were then dried in the vacuum oven at 50 °C for 72 hours. The samples were then stored in petri glass dishes for further analysis. The G-series products turned

out to be very brittle, much like the E-series samples. They also were slightly pink in color, due to the strong pink color of the RAFT agent. **Table 3** shows the compositions of G series samples.

**Table 3.** Compositions of G-Series polyacrylamide samples, showing grams of RAFT agent, initiator, and acrylamide, with product yield, theoretical yield, and percent yield.

Samples G1-G6	2-Cyano-2-propyl benzodithioate (g):	Acrylamide (g):	4,4'-AZO-bis-(4-cyano-valeric acid) (g):	Product (g):	Theoretical Yield (g):	Percent Yield (%)
1G	0.0056	0.2132	0.0041	0.1778	0.2229	80
2G	0.0054	0.2132	0.0044	0.1370	0.2230	61
3G	0.0113	0.2132	0.0042	0.1224	0.2287	54
4G	0.0111	0.2132	0.0043	0.1034	0.2286	45
5G	0.0226	0.2132	0.0043	0.1751	0.2401	73
6G	0.0224	0.2132	0.0043	0.1095	0.2399	46

### Microwave Synthesis

A plot showing the temperature graphed against time with power and pressure constraints of the microwave synthesis for G-Series are shown in **Figure 13** below.

**Figure 14** illustrates the specifics of the parameters in the microwave-assisted synthesis.

# Anton Paar Multiwave 5000

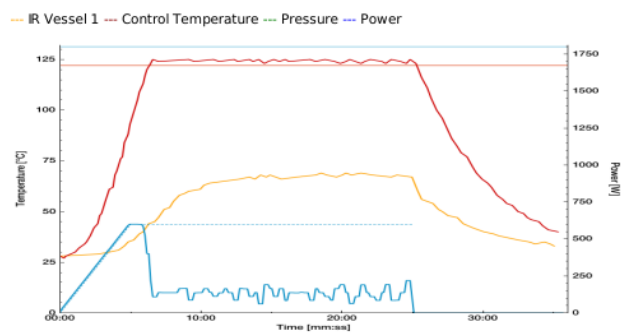
## Experiment Report

Serial Number: 83061639      Software Version: 1.0.6625.19-Release  
Configuration: 00110010  
Name: -      Location: -

## Processing Protocol

Name: 20210318-1637\_121      Date: 03/18/2021 16:38:27  
User at start: Administrator      User at end: Administrator  
Consecutive Number: 121  
Unique ID: 791ff548-b6a4-4e80-8a28-11cce5ad3ee5

## Graph



## Vessels 1 - 4

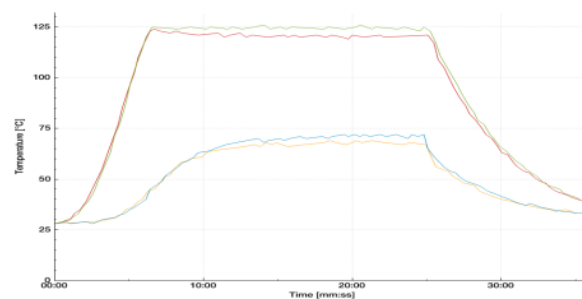


**Figure 13.** Energy and Temperature plots of G-Series Microwave synthesis.

### Method Settings

Name: Hannah Rotor: Rotor 4X24MG5  
Application Group: Synthesis Category: Polymers  
Program Type: Power Vessels: 2  
Cooling Temperature [°C]: 40 Cooling Fan Level: 3

### Limits

Power Limit [W]: 1800  
IR Limit [°C]: 122

### Steps

Step No	Power [W]	Time [hh:mm:ss]	Fan Level
1	600	00:05:00	1
2	600	00:20:00	1

### Recipe

AM + Val RooR + water

### Experiment Result

Status: Success  
Total Runtime: [hh:mm:ss] 00:35:38  
Controller State: L

### Maxima

Max. Internal T [°C]: 125.9  
Max. power [W]: 600  
T Vessel 1 [°C]: 69  
T Vessel 2 [°C]: 124  
T Vessel 3 [°C]: 72  
T Vessel 4 [°C]: 126  
Max. Tmag1 [°C]: 55  
Max. Tmag 2 [°C]: 54  
Max. Current [A]: 8.8

.....  
Date (Signature)

**Figure 14.** Parameters of microwave synthesis polymerization for G Series.

## **C. Analysis Methods**

### **1. Thermogravimetric Analysis**

Samples from the A, E and G series were analyzed by thermogravimetric analysis using a TA Q500. The samples were cut or ground into a rough powder, then approximately 0.010g, (5-15 mg) of the samples were weighed out and placed on platinum pans. They were then heated to 1000 °C at a rate of 10 °C/min under nitrogen gas.

### **2. DSC Analysis**

TA Instrument DSC Q2000 was used to analyze the sample using differential scanning calorimetry. The samples were weighed out between 2 and 3 mg on an analytical balance, then crimped into T-Zero Low Mass hematic aluminum pans. The sample and reference pans were heated at a rate of 10 °C/min to 170 °C under a nitrogen purge.

### **3. Fourier Transform Infrared (FTIR) Spectroscopy**

Samples were prepared for FTIR analysis by crushing to a fine powder with a ceramic mortar and pestle. The molecules were fine enough to have acceptable surface contact on the ATR. Scan parameters included 64 scans, 4.00 cm<sup>-1</sup> resolution, and automatic atmospheric suppression. iS50 ATR sample compartment, DTGS ATR detector, XT-KBr beam-splitter, and IR source were used. Background samples were

collected before each run, and the final spectra were processed with both baseline correction and ATR correction.

#### **4. NMR Analysis**

To characterize using NMR, the samples were dissolved in D<sub>2</sub>O. The concentration of sample in D<sub>2</sub>O solution varied through the different series. Series A NMR solution initially had a 5% weight ratio, but that was much too viscous to properly place in NMR tubes, so it was reduced to 1% weight ratio. Series E samples were prepared using a 1% weight ratio. G Series samples were also prepared at a 1% weight ratio, however, the noise to signal ratio was too high to properly evaluate the spectra, so a 3% weight ratio sample was prepared, which had better signal-to-noise ratio of the peaks. <sup>1</sup>H and <sup>13</sup>C spectra were obtained on a JEOL ECA 500 MHz spectrometer using automated methods. <sup>13</sup>C NMR spectra required 16,384 scans for analysis. <sup>1</sup>H NMR spectra required 64 scans.

#### **5. Dilute Solution Viscosity Analysis**

A Koehler Kinematic Viscosity Bath was used to measure the dilute solution viscosity of each sample. The process of viscosity analysis started with dissolving enough sample in a 25 mL volumetric flask to make a 0.1 g/dL concentration. According to literature, an ideal concentration would have been 1 g/dL.<sup>28</sup> However, the 1 g/dL solution proved to be much too viscous to flow through the viscometer. 0.4 g/dL solutions were also attempted, but those were too viscous as well. Individually, twelve milliliters of the sample solutions were pipetted into the viscometer, then sat for 10 minutes to equilibrate. Afterwards, three runs of the pure 0.1 g/dL solution were timed. Two milliliters of DI

H<sub>2</sub>O were then added with mixing to the solution, which sat for 5 minutes to equilibrate.

The process repeated until 10 mL of DI H<sub>2</sub>O were added. **Table 4** and **Table 5** below show an example of the viscosity measurements and calculations.

**Table 4.** Viscosity tests solution concentrations and time measurements of A5 sample.

Run:	Time (s):	Concentration (g/dL):
1	178.81	12ml
2	178.95	0.100
3	179.02	
1	163.97	+2 ml H2O
2	164.15	0.086
3	164.03	
1	154.73	+4 ml H2O
2	153.44	0.075
3	153.58	
1	145.26	+6 ml H2O
2	145.39	0.067
3	145.37	
1	139.09	+8 ml H2O
2	138.99	0.060
3	139.03	
1	134.27	+10 ml H2O
2	134.40	0.054
3	134.18	

**Table 5.** Viscosity tests solution concentrations and calculations based off time measurements of sample A5.

Concentration (g/dL):	Average T (s):	Relative Viscosity ( $\eta_r = t/t_0$ )	Specific Viscosity ( $\eta_{sp} = (t-t_0)/t_0$ )	Reduced Viscosity ( $\eta_{red} = \eta_{sp}/C$ )	Inherent Viscosity ( $\eta_{inh} = \ln \eta_r/c$ )
0.100	178.93	1.80	0.80	8.05	2.89
0.086	164.05	1.65	0.65	7.61	2.96
0.075	153.92	1.55	0.55	7.37	3.03
0.067	145.34	1.47	0.47	6.95	3.09
0.060	139.04	1.40	0.40	6.71	3.15
0.054	134.28	1.35	0.35	6.56	3.22
	$t_0$ (sec) =	<b>99.15</b>			

## CHAPTER III: RESULTS AND DISCUSSION

Two different products were synthesized using free-radical polymerization, polyacrylamide and poly(acrylamide-co-diallyldimethylammonium chloride). One product was formed using reversible addition-fragmentation chain transfer polymerization (RAFT) through microwave-assisted synthesis, which was polyacrylamide. The products were then characterized through several methods. These included nuclear magnetic resonance (NMR), Fourier transform infrared spectroscopy (FTIR), and dilute-solution viscometer tests. Thermogravimetric analysis (TGA) and differential scanning calorimetry (DSC) were used to evaluate the thermal properties of the compounds.

### A. FTIR

**Figures 15-17** show FTIR overlay spectra from the samples created in A Series, E Series, and G Series. **Figure 18** shows a stack plot of a sample from each of the three series for comparison. The following two figures, **Figures 19 and 20**, show zoomed-in stack plots of the three series in regions ( $550\text{-}1900\text{ cm}^{-1}$ ) and ( $2380\text{-}3850\text{ cm}^{-1}$ ) for a closer inspection. Finally, **Figures 21** specific peak assignments for Series A. The specific peak assignments for Series E and G can be found in the **Appendix. Table 6** provides the peak assignments as well as the corresponding functional groups.

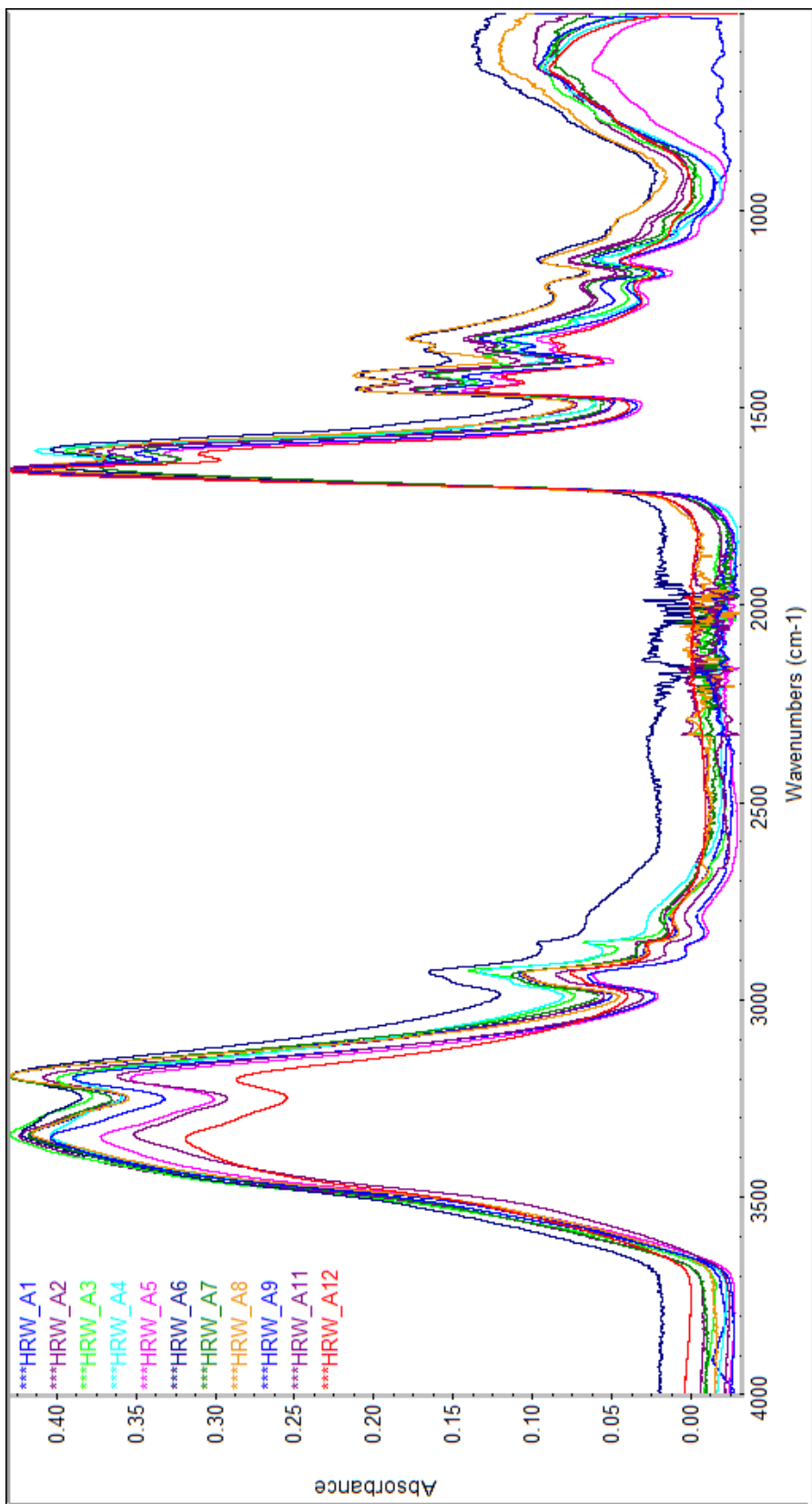


**Figure 15:** FTIR overlay plots of A Series

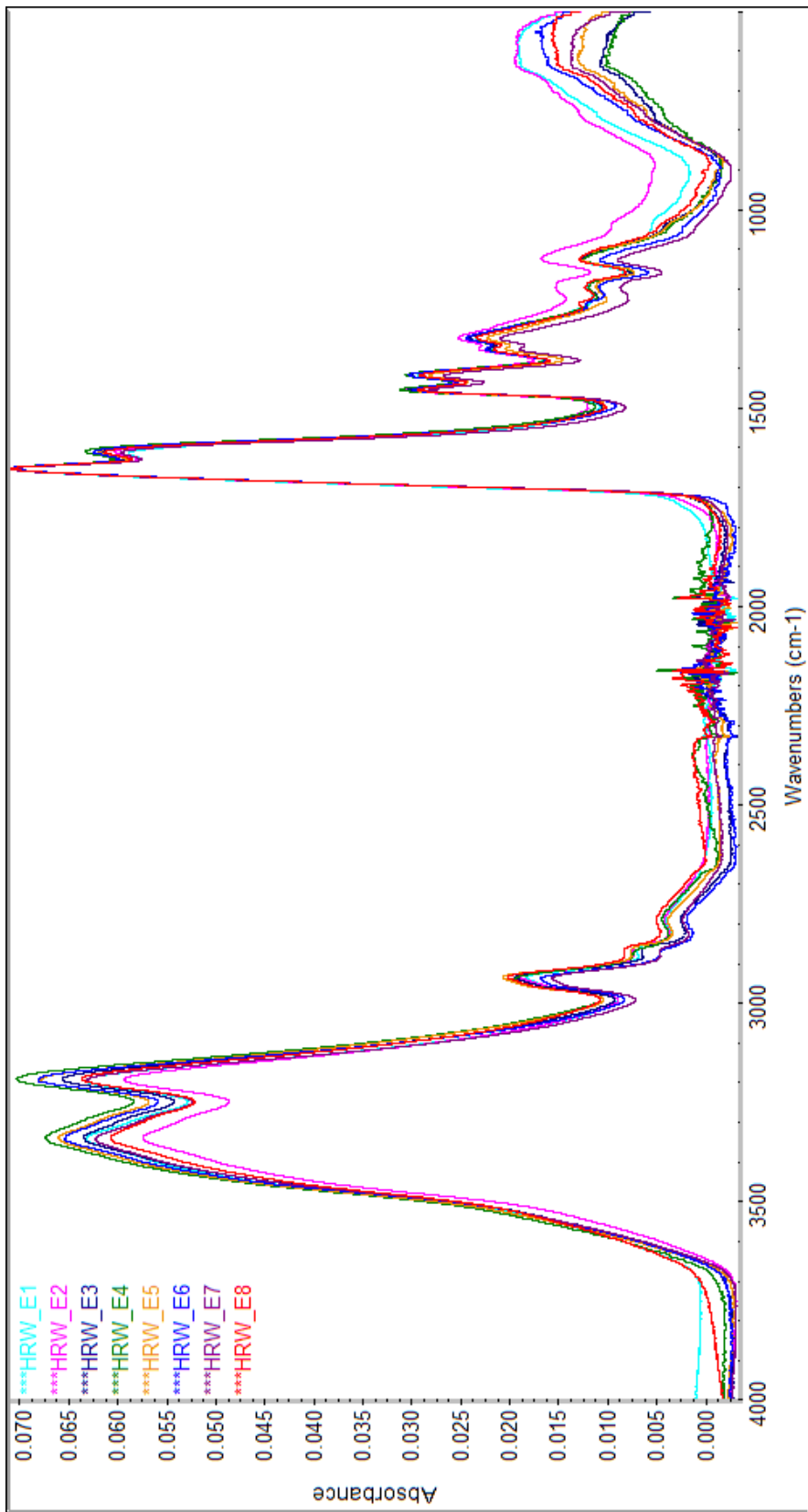
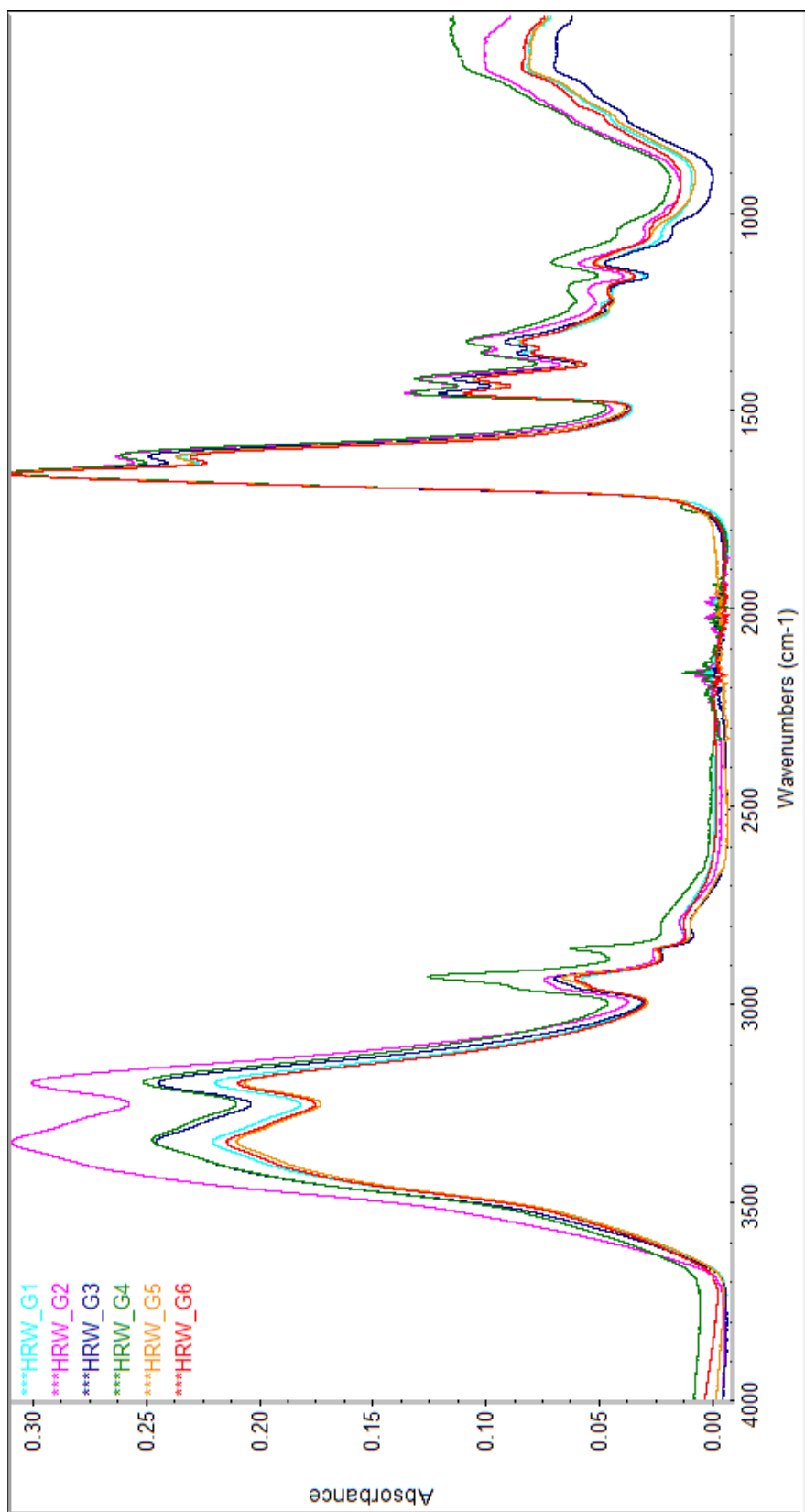
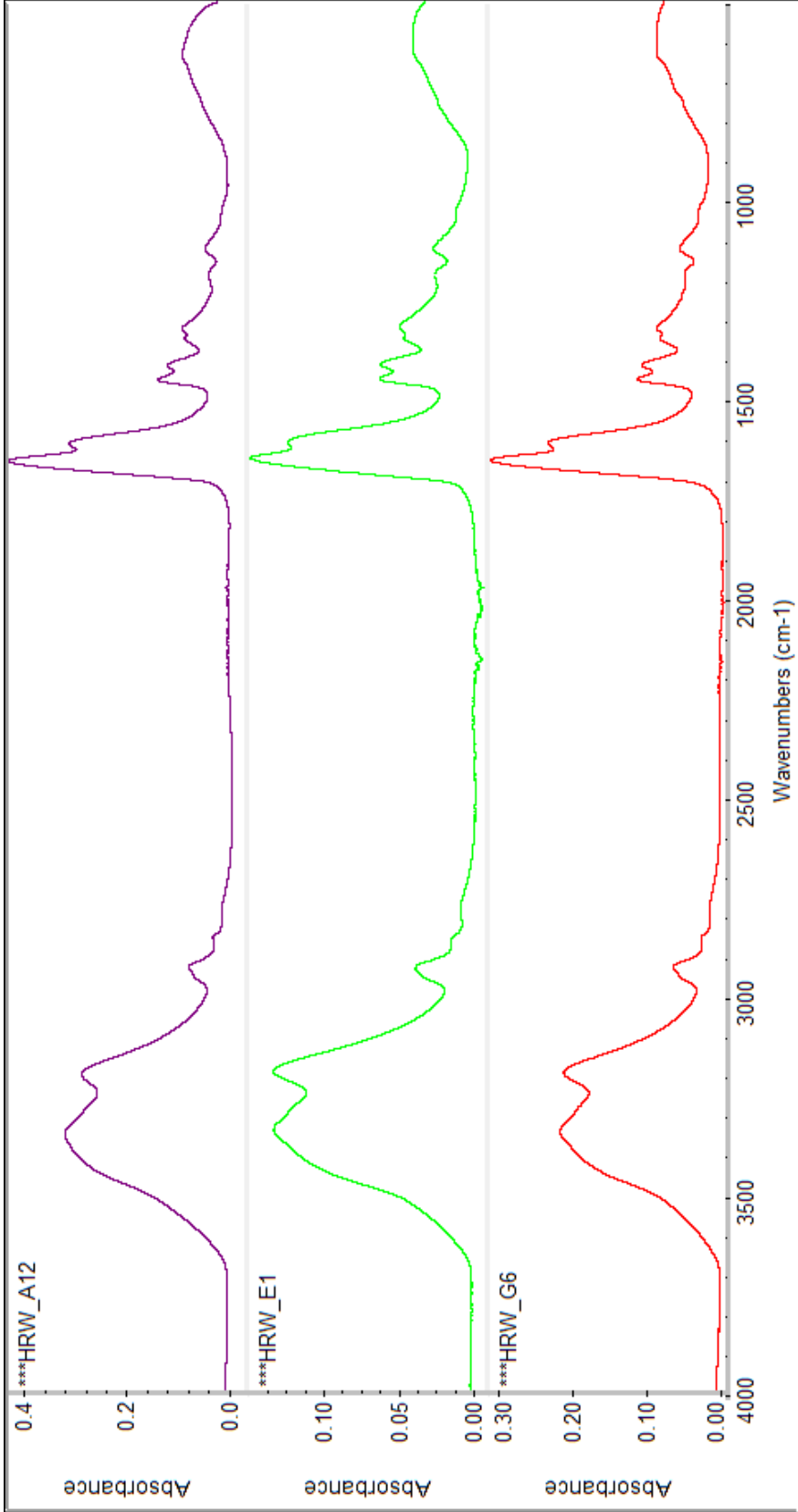


Figure 16: FTIR overlay plots of E Series



**Figure 17:** FTIR overlay plots of G Series.



**Figure 18:** FTIR stack plots of A Series, E Series, and G Series.

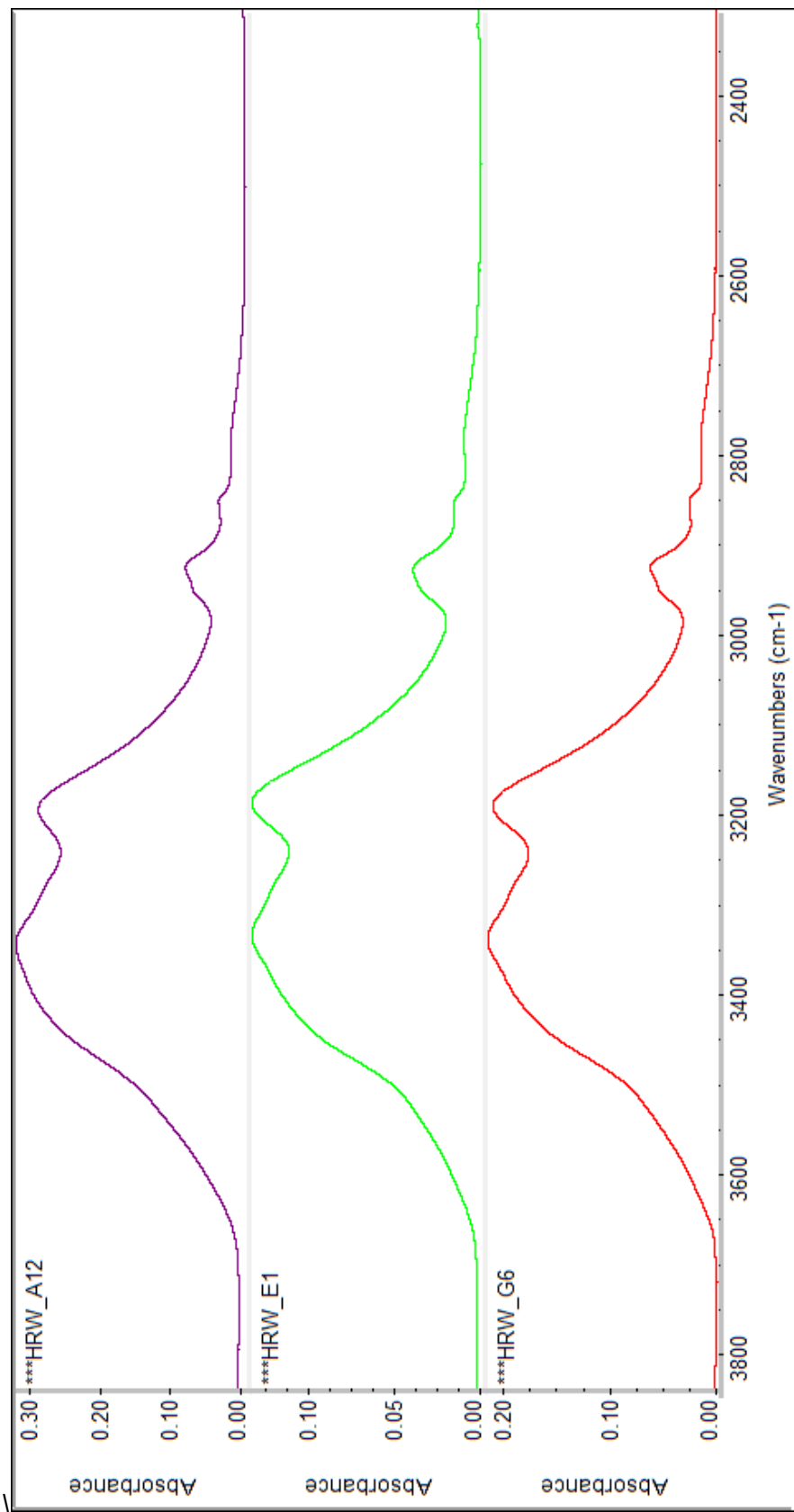


**Figure 19:** FTIR stack plots of A Series, E Series, and G Series. (2380-3850cm<sup>-1</sup>)

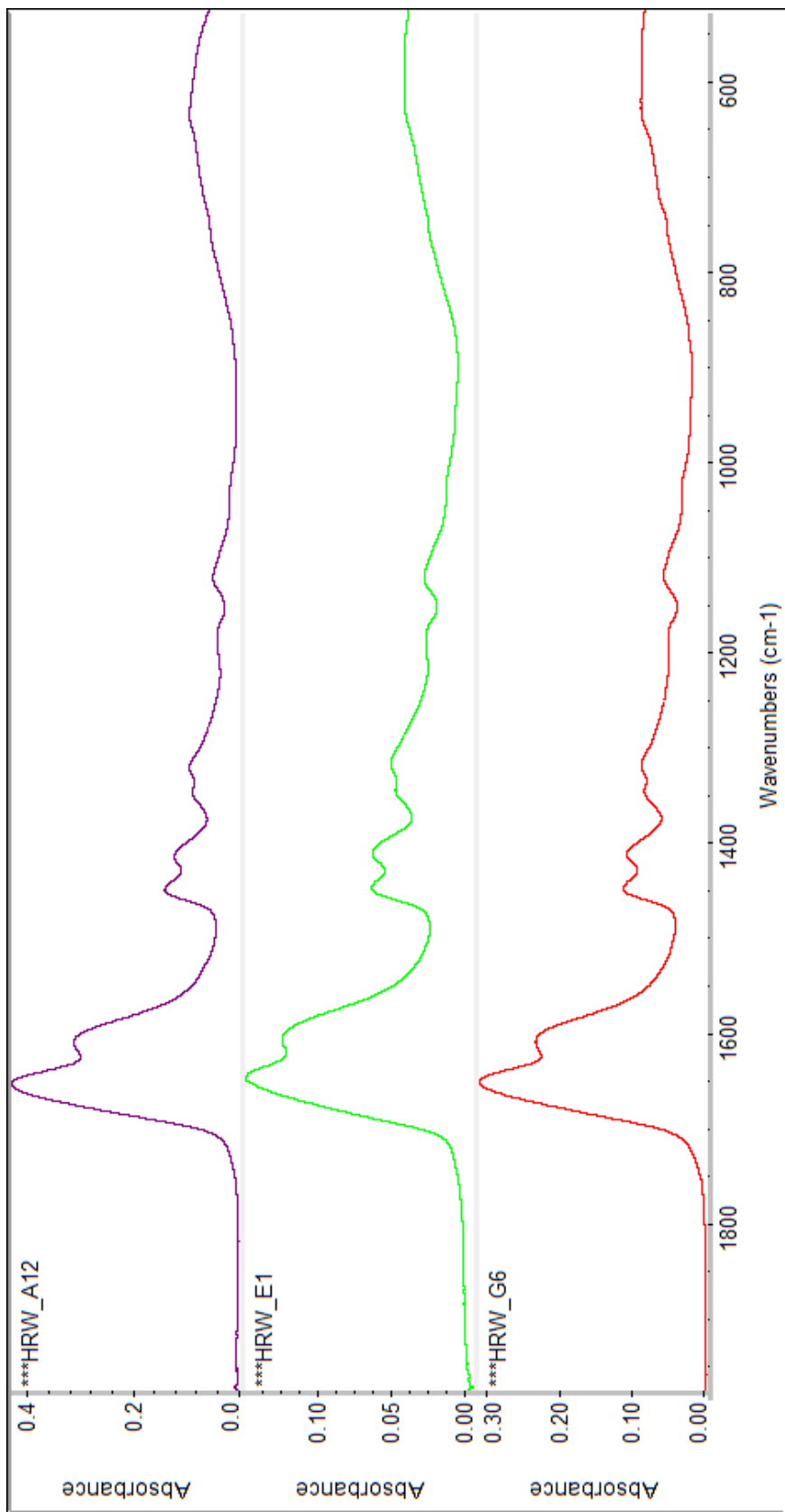


**Figure 20:** FTIR stack plots of A Series, E Series, and G Series. (550-1900cm<sup>-1</sup>)

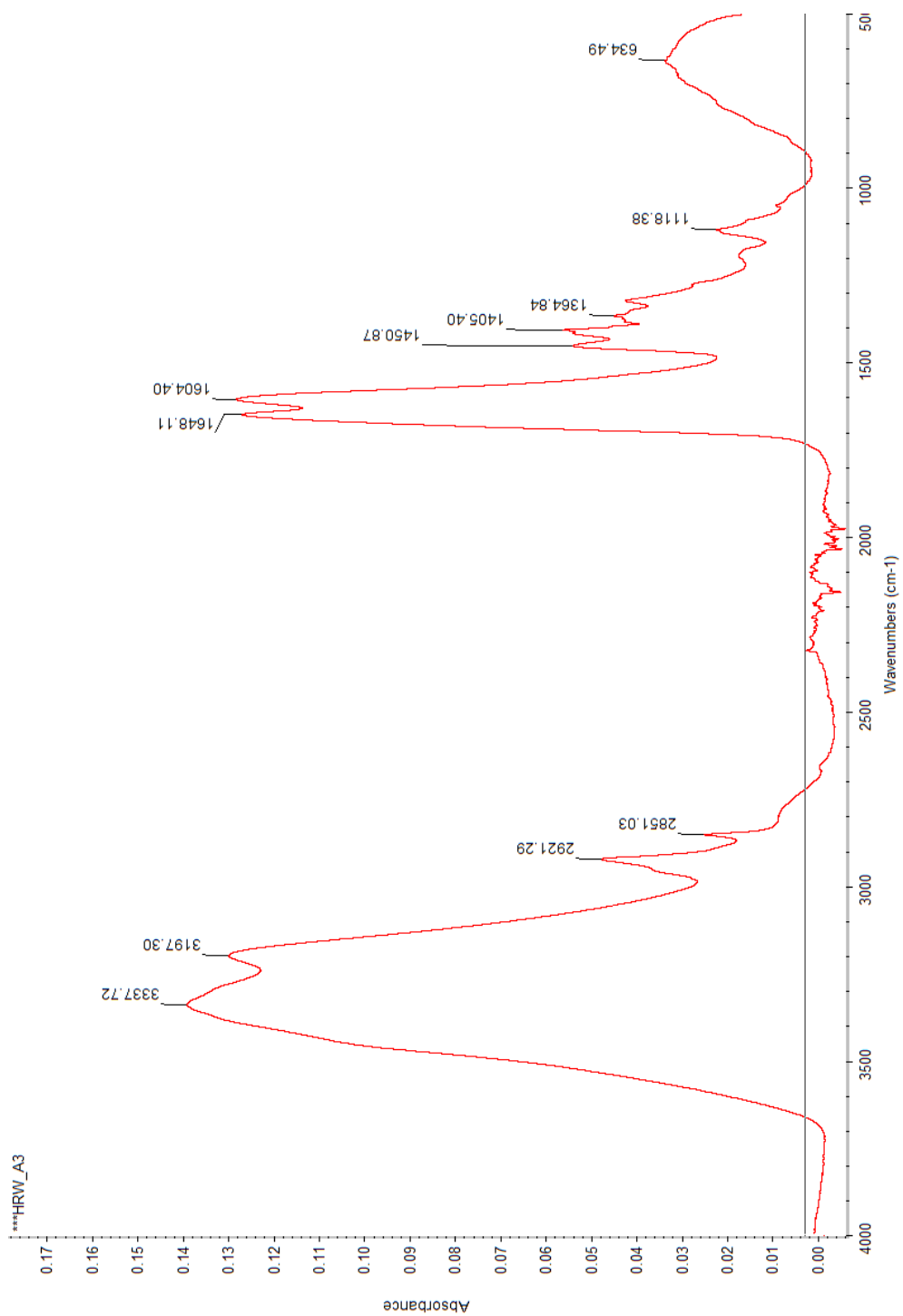


**Figure 21:** FTIR plots Sample A3 specific peak assignments

**Table 6.** Peak Assignments for A3, E8, and G4 samples with corresponding functional groups.

Series A: (cm <sup>-1</sup> )	Series E:(cm <sup>-1</sup> )	Series G:(cm <sup>-1</sup> )	Group
3337.72	3336.86	3337.76	primary amide asymmetric stretching band NH <sub>2</sub>
3300-3250	3300-3250	3300-3250	secondary amide N-H stretching
3197.3	3186.57	3189.45	primary amide NH <sub>2</sub> symmetric stretching
3100-3060	3100-3060	3100-3060	secondary amide II overtone
2921.29	2929.5	2924.24	symmetrical CH <sub>2</sub> stretch, chain
2851.03	x	2853.12	asymmetrical C-H stretching
1648.11	1648.27	1650.44	primary amide C=O stretching
1604.4	1606.54	1606.69	Secondary amide C=O stretching
1450.87,1405.40	1449.37,1413.02	1449.95,1413.58	CH <sub>2</sub> scissor

The IR spectra support the hypothesized Series A and G polyacrylamide structures. The broad peaks in the 3000-3400 cm<sup>-1</sup> are linked to N-H bonds in the amide of the molecule. Primary asymmetric amide stretching peaks are seen around 3337 cm<sup>-1</sup>, and primary amide symmetric stretching is seen around 3190 cm<sup>-1</sup>. Interestingly, this peak has a significantly higher value in the A series than the E and G series. Secondary amide stretching shows up around 3300-3250 cm<sup>-1</sup> in all the series. The C-H interactions are evident in the 2800-2900 cm<sup>-1</sup> range, while C=O interactions show up quite clearly in the 1600-1650 cm<sup>-1</sup> range. There are a few peaks near the fingerprint region that may be CH<sub>2</sub> scissoring. The peaks around 1450 cm<sup>-1</sup> and 1410 cm<sup>-1</sup> in the E series are from the lack of -CH in -N(CH) symmetrical bending vibration absorption peak, and an N-CH stretching vibration peak, respectively. These show that a DADMAC monomer is present. 1451.60 cm<sup>-1</sup> is the absence of -CH<sub>3</sub> in -N<sup>+</sup>(CH<sub>3</sub>)<sub>3</sub> symmetrical bending vibration absorption peak, while 1414.54 cm<sup>-1</sup> is N-CH<sub>3</sub> stretching vibration peak, thus illustrating the existence of DADMAC monomer.<sup>29</sup> Another telling sign that the E series contained DADMAC was the lack of peak at around 2900 cm<sup>-1</sup>, which matches acrylamide-DADMAC polymer IR in previous literature.<sup>30</sup>

## B. NMR

The  $^{13}\text{C}$  and  $^1\text{H}$  spectra for Series A, E, and G are shown in **Figures 24-29**. Zoomed-in spectra are available in the **Appendix** for closer analysis.

The  $^1\text{H}$  NMR of all three series is comparable to spectra from previous literature, proving that the hypothesized products were correctly synthesized.<sup>29,30</sup> Specific peak assignments for  $^1\text{H}$  NMR are given to molecules pictured on **Figures 25,27, and 29**.  $^{13}\text{C}$  NMR is portrayed in **Figures 24,26, and 28**. **Table 7** illustrates the peak integrals, relative shifts, and corresponding structures of the  $^1\text{H}$  NMR spectra.

**Table 7.**  $^1\text{H}$  NMR Peak Assignments of Samples A8, E4, and G4.

Sample A8			Sample E4			Sample G4		
Shift (ppm)	Integration Values	Comments	Shift (ppm)	Integration Values	Comments	Shift (ppm)	Integration Values	Comments
4.6	25	D <sub>2</sub> O	4.60	50	D <sub>2</sub> O	4.6	6	D <sub>2</sub> O
2.1	2	C-H hydrogen	3.60	0.15	CH <sub>2</sub> hydrogens on DADMAC nitrogen-based ring	2.1	7	C-H hydrogen
1.5	3	C-H <sub>2</sub> chain hydrogen	3.10	1.2	CH <sub>3</sub> hydrogens on DADMAC nitrogen-based ring	1.5	1	C-H <sub>2</sub> chain hydrogen
			2.50	0.2	CH <sub>1</sub> hydrogens on DADMAC nitrogen-based ring			
			2.00	2	Acrylamide CH			
			1.50	3	chain CH <sub>2</sub>			

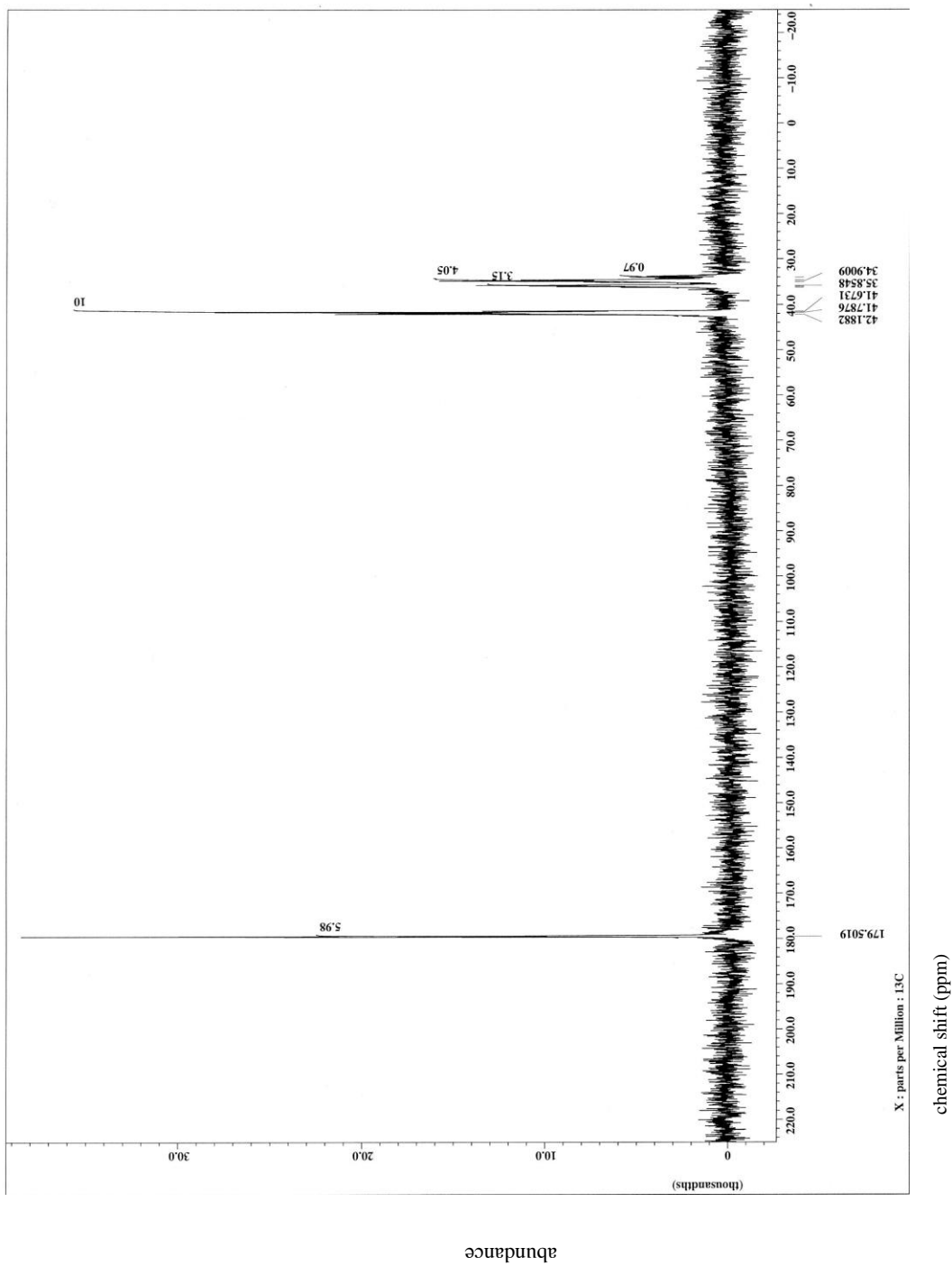


**Figure 22.**  $^{13}\text{C}$  NMR ( $\text{D}_2\text{O}$ ) Sample A8

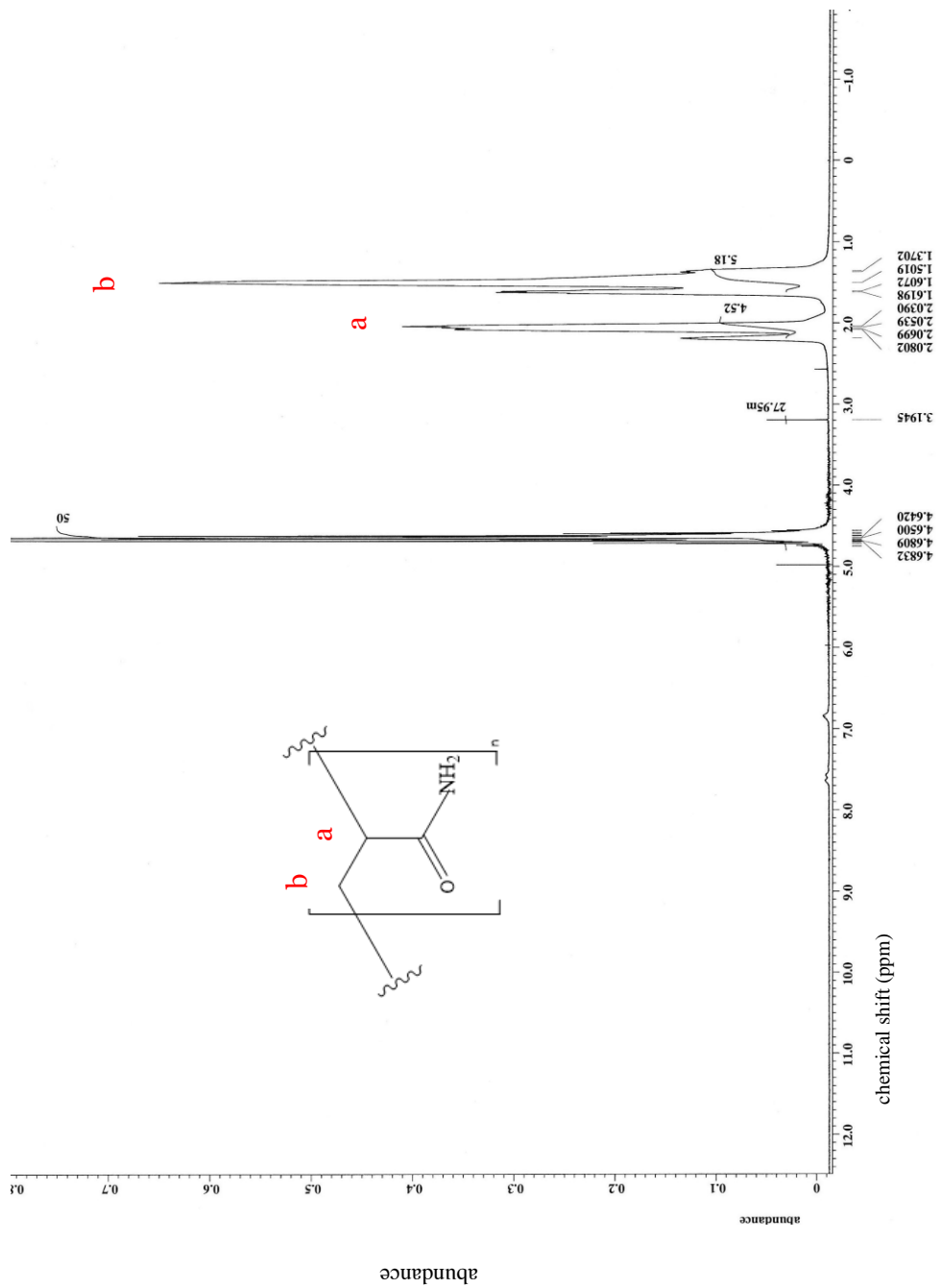
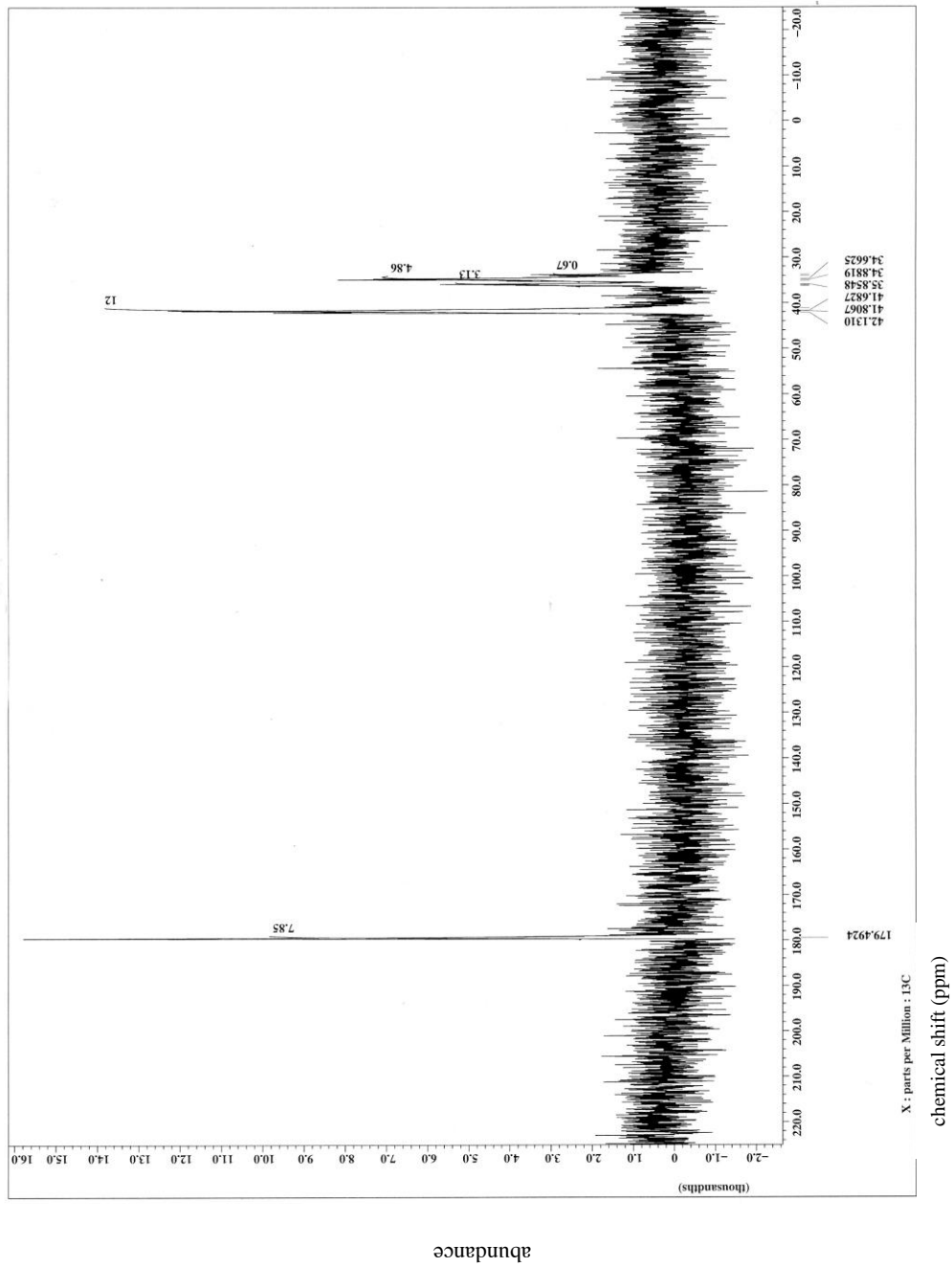
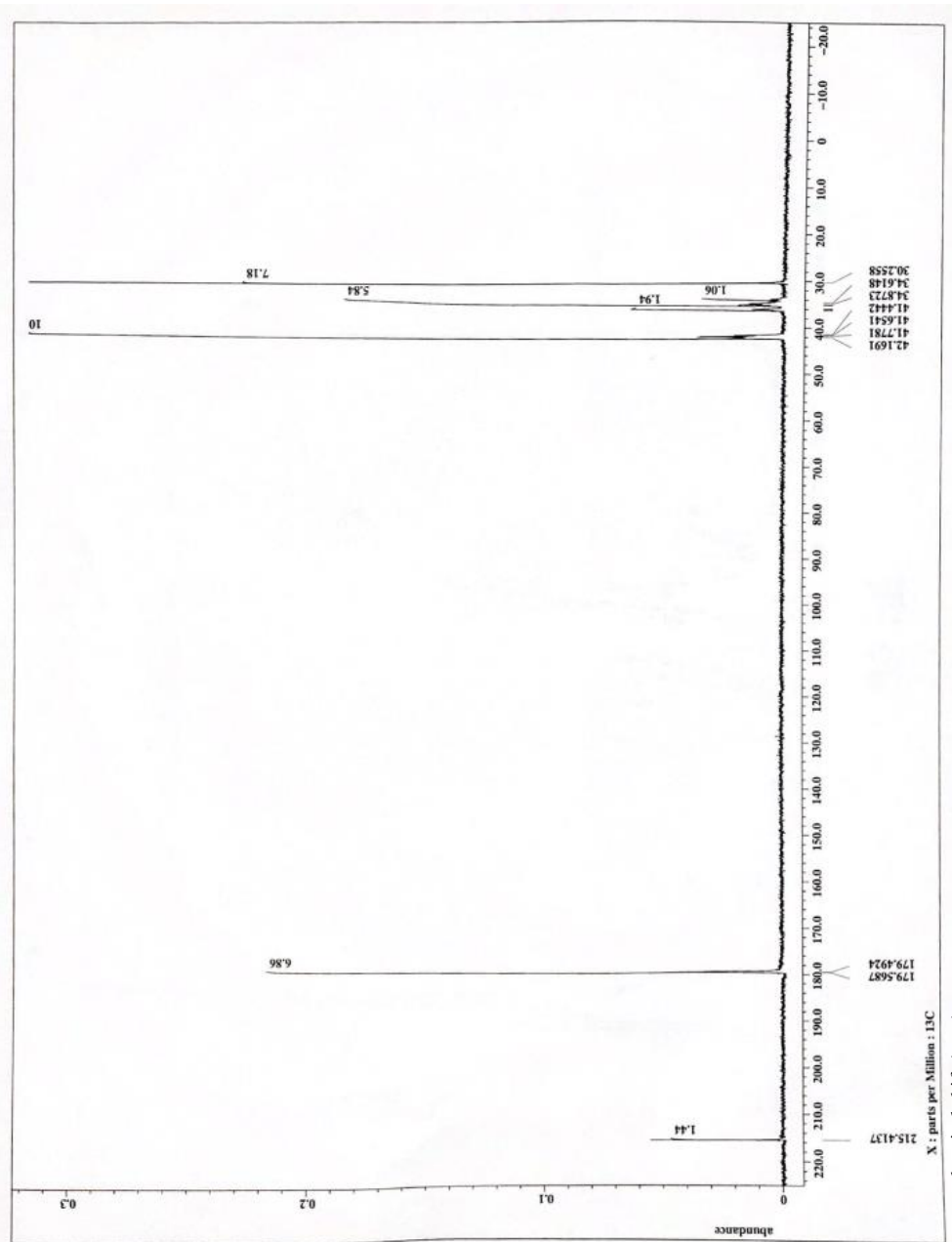


Figure 23. <sup>1</sup>H NMR (D<sub>2</sub>O) Sample A8



**Figure 24.**  $^{13}\text{C}$  NMR ( $\text{D}_2\text{O}$ ) Sample E4





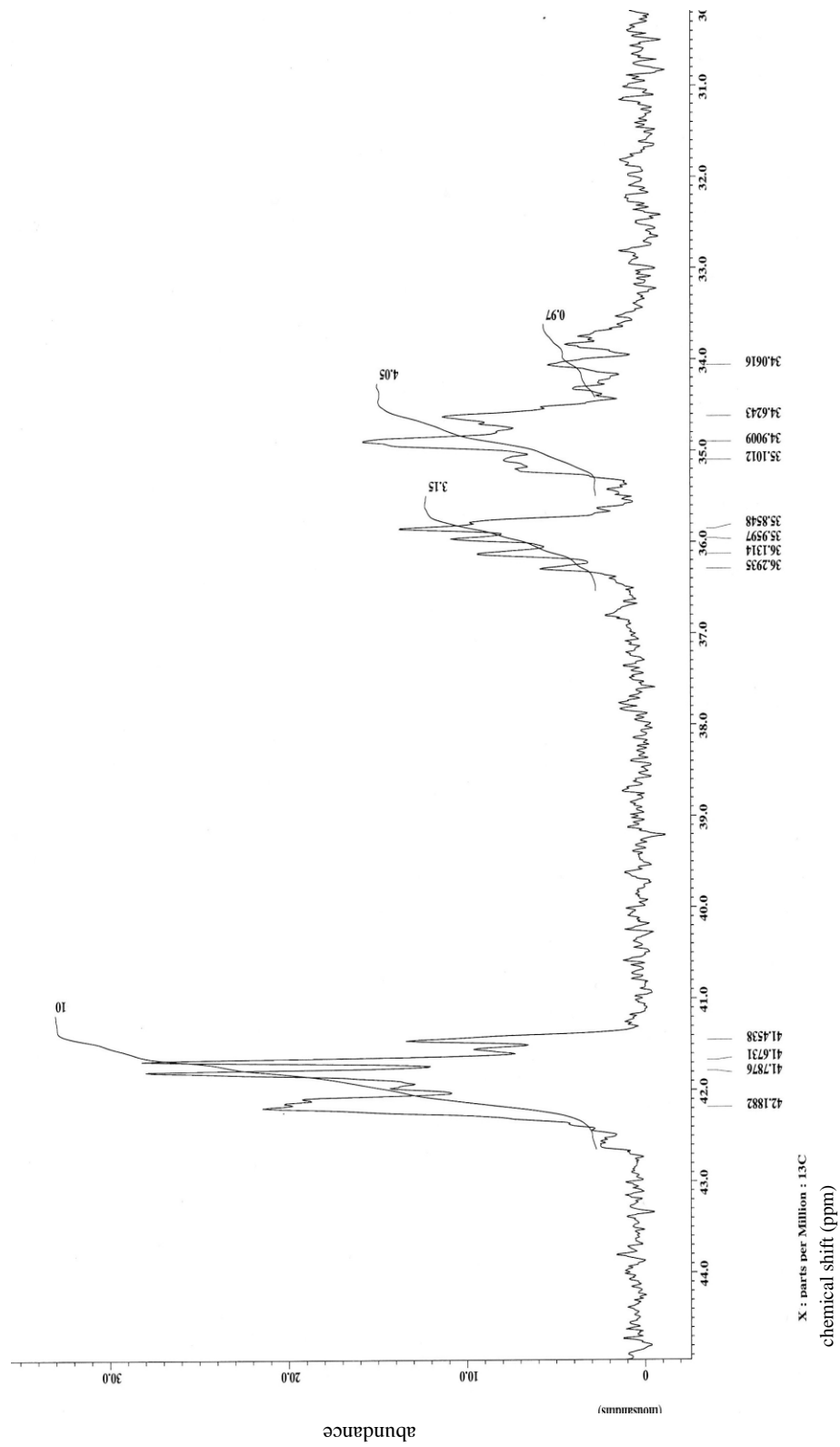
abundance

Figure 26.  $^{13}\text{C}$  NMR ( $\text{D}_2\text{O}$ ) Sample G4



$^1\text{H}$  NMR was primarily used to confirm the structures of the product samples. The spectra for Samples A8 and G4 clearly showed the hydrogens of a polyacrylamide. The H-atom bonded to the tertiary carbon in the amide had a peak shift of approximately 2.1 ppm, and the H-atom on the secondary carbon atom had an approximate peak shift of 1.5 ppm in both spectra. The solvent,  $\text{D}_2\text{O}$ , was depicted at 4.6 ppm. The  $\text{NH}_2$  hydrogen peaks usually do not appear because heteroatoms such as N-H can exchange rapidly with the solvent, even more so if it is  $\text{D}_2\text{O}$ . However, the little blips at 6.5-8 ppm on the A8  $^1\text{H}$  NMR spectra are due to the amide hydrogens. Notably, the main difference in the Series A and Series G  $^1\text{H}$  NMR spectra seems to lie in the integration values. For Sample A8, the ratio of C-H hydrogens to C-H<sub>2</sub> hydrogens is 2:3, but for Sample G4 it is 7:1. Integration values represent the relative amount of hydrogens present in the same chemical environment. The discrepancy between the spectra of the free-radical polymerization, A8, and the controlled-radical polymerization, G4, could be due to contrasting molecular structures created in the two syntheses. The  $^1\text{H}$  NMR spectra for Sample E4 was consistent with the molecular composition of poly(acrylamide-co-diallyldimethylammonium chloride). Peaks at 3.60, 3.10, and 2.50 ppm show  $\text{CH}_2$  hydrogens,  $\text{CH}_3$  hydrogens, and CH hydrogens in the DADMAC co-monomer, respectively. Peaks at 2.00 ppm and 1.50 ppm are caused by the acrylamide co-monomers (also seen in A8 and G4 spectra). The  $^{13}\text{C}$  NMR spectra obtained was not as useful in determining distinctions between the series. The noise-to-signal ratio was too large to differentiate between some of the smaller peaks, inhibiting confident specific peak assignments. Unfortunately, even 16,384 scans and ~13-hour runs were not adequate in lessening the spectra noise. The problem lay in how viscous the samples were when a

higher concentration was used. The samples proved to be too viscous to transfer to NMR tubes unless at a relatively low concentration. Solutions to this hinderance may include adding a relaxing agent to speed up the run times, or using even more scans per sample. However, we were able to compare the tacticities between the A series and G series. Specifically, the effects the two syntheses, free-radical and controlled-radical polymerization, had on the stereochemistry of the molecules were studied. Free-radical synthesis usually creates amorphous, atactic polymers. The mm, mr, and rr triad sequences represent isotactic, atactic, and syndiotactic parts of the polymer chains, respectively. Controlled-radical synthesis may result in slightly more uniform tacticities. The peak integrals of the  $\beta$ -carbon (methylene) were compared, which would appear in between  $\sim 34 - 36.6$  ppm of the  $^{13}\text{C}$  NMR spectra. A closer look at this region in the  $^{13}\text{C}$  NMR spectra of Samples A8 and G4 are shown in **Figures 28 and 29**. A comparison of the integral values is shown in **Table 8**. The peak at around 30 ppm could be due to RAFT agent present in the mixture.



**Figure 28.** Zoomed-In  $^{13}\text{C}$  NMR ( $\text{D}_2\text{O}$ ) Sample A8

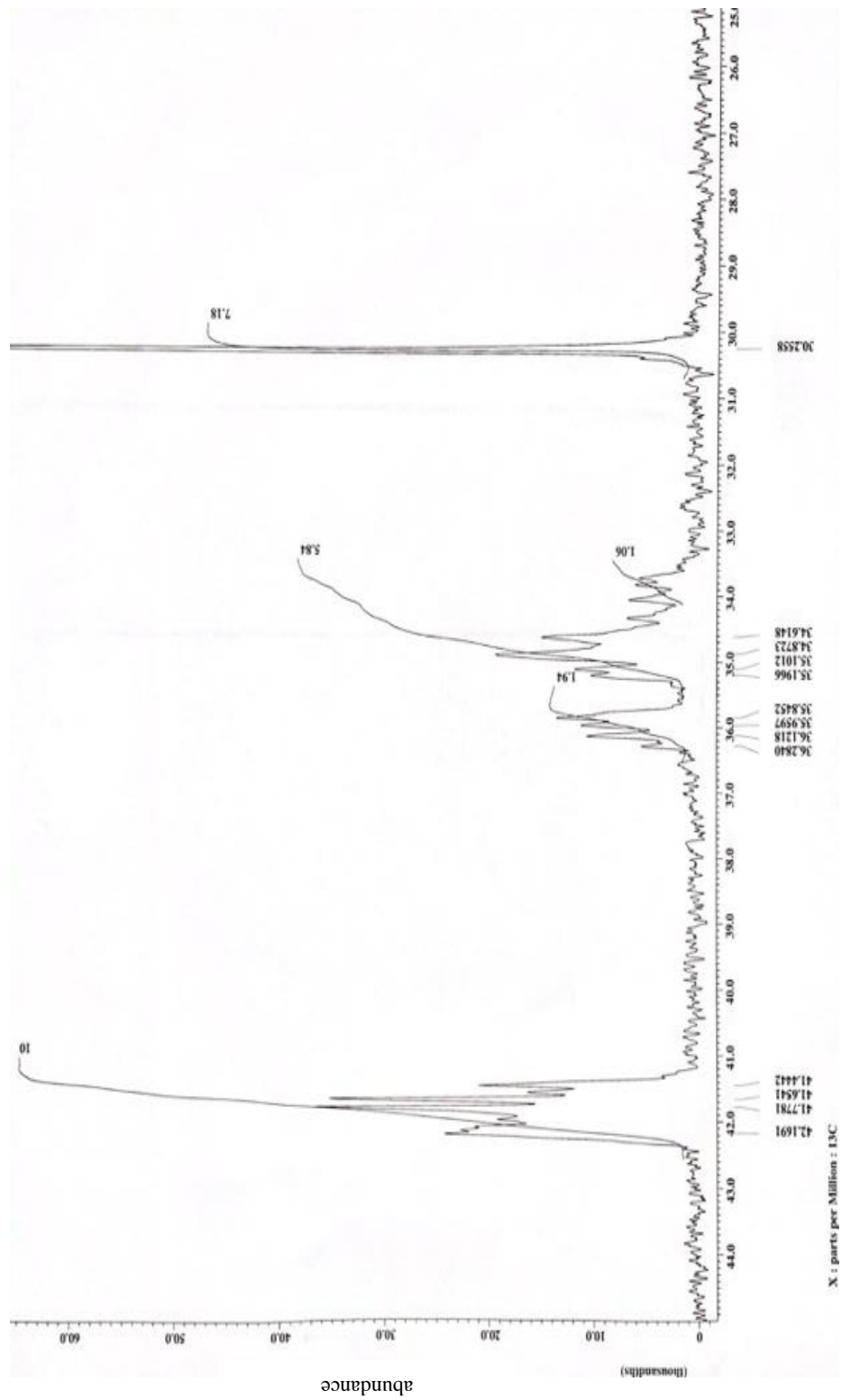


**Figure 29.** Zoomed-In <sup>13</sup>C NMR (D<sub>2</sub>O) Sample G4

**Table 8.** Comparison of Tacticities between  $^{13}\text{C}$  NMR Samples A8 and G4.

<b>Methylene Carbon:</b>	<b><i>mm/mr/rr</i></b>	<b><i>Percentage mm/mr/rr</i></b>
<b>A8</b>	<b>3/5/1</b>	<b>33/56/11</b>
<b>G4</b>	<b>2/6/1</b>	<b>22/67/11</b>

### C. Thermogravimetric Analysis

**Figure 30** portrays an overlay plot of the thermal decomposition of four A-series samples. **Table 9** contains the onset of degradations of A, E, and G series. TGA overlay plots of E series and G series can be found in the **Appendix**. Samples in the individual series were chosen based on the amount of initiator they had, choosing samples with the lowest and highest amount of initiator to see if it would affect the molecular decomposition.

**Table 9.** Degradation Onsets of Series A, E, and G.

<b>Sample</b>	<b>1st onset of degradation (°C)</b>	<b>2nd onset of degradation (°C)</b>	<b>3rd onset of degradation (°C)</b>
A2	198.35	265.75	396.88
A12	186.44	262.58	403.79
E2	263.14	358.52	x
E4	221.18	263.25	406.51
G2	173.96	254.48	394.24
G6	177.05	247.89	390.83

Thermogravimetric analysis of the samples shows some interesting trends in the polymer samples. Thermogravimetric analysis tracks the weight percentage of the sample at continuously increasing temperatures. Through these measurements, it can be determined at what temperatures molecules break down, and how much weight they lose as a result. Series A and Series G samples had lower temperatures at their first onset of degradation; samples A2 and A12 had temperatures between 180-190°C while samples G2 and G6 had temperatures in the 170-180°C range. In contrast, E2 and E4 had temperatures above 200°C. The same trend in temperatures occurs at the 2<sup>nd</sup> and 3<sup>rd</sup> onsets of degradation. The maximum rate of decomposition occurs at the third onset of degradation, around 390-410°C for all series. Plot lines were graphically offset to allow for better analysis. Of the samples, E Series seems to be the most thermally stable. Thermal stability depends on the amount of heat required to break the compound. The stronger the bonds between the atoms are, the more heat will be required to break them.

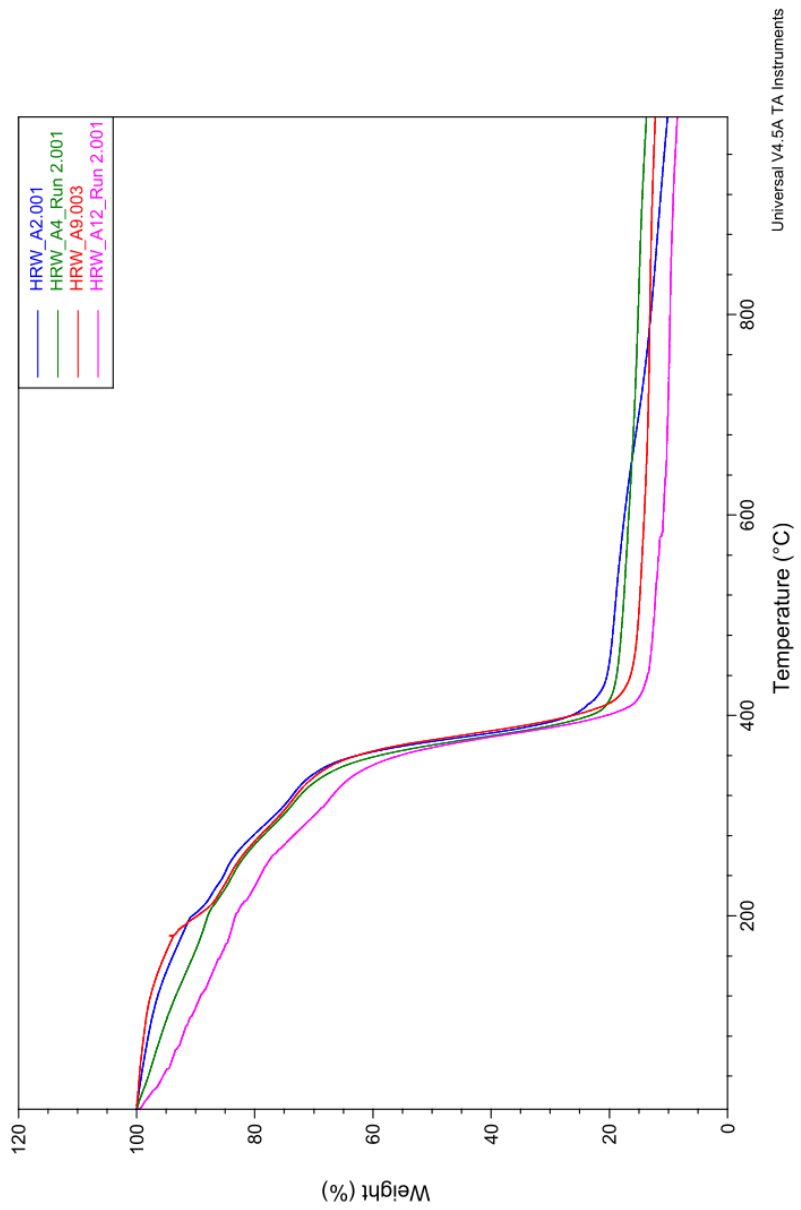


Figure 30. Overlay Plot of TGA thermogram for A Series.

## D. Differential Scanning Calorimetry

**Table 10** shows the glass transition temperature, the melting points, and the heat of fusion related to the melting points for Series A-G. **Figure 31** is an overlay plot of the DSC runs.

**Table 10.**  $T_g$ ,  $T_m$ , and Heat of Fusion for Series A, E, and G.

Sample	1 <sup>st</sup> $T_g$ (°C)	2 <sup>nd</sup> $T_g$ (°C)	1 <sup>st</sup> M.P.(°C)	Heat of Fusion 1st M.P. (J/g)	2 <sup>nd</sup> M.P.(°C)	Heat of Fusion 2nd M.P.	3 <sup>rd</sup> M.P.(°C)	Heat of Fusion 3rd M.P.
A2	76.73	x	159.41	4.906	164.02	14.070	x	x
A12	68.86	132.68	132.68	0.248	155.30	2.697	160.18	42.70
E2	66.20	x	115.21	77.120	x	x	x	x
E4	65.10	130.87	147.86	2.330	153.79	1.024	x	x
G2	57.43	114.39	144.64	6.113	152.27	7.989	x	x
G6	48.15	94.33	143.72	3.979	147.37	1.186	166.44	2.18

Differential Scanning Calorimetry is used to examine the conditions in which materials change states of matter. For this analysis, two pans are heated equivalently. One is a reference pan and the other holds the sample. The process of changing from one state to another can quickly change the rate of heat a sample absorbs. As a result, when comparing the temperature differences to a steadily heating reference pan, points of glass transitions and melting temperatures can be determined. In most of the samples, it was clear there were two glass-transition points (all except for A2 and A12). A glass transition point occurs when an amorphous sample changes from a “glassy”, hard, brittle solid into a more viscous state. Melting points occur when distinct forms of material change from the solid to liquid phase. If a sample has several melting points, it could mean there were several types of crystalline structures in the sample, breaking bonds at

different temperatures. This is apparent in most of the samples as well. The peak temperature used for the series, 170°C, was obtained from the averages of the first onsets of degradation in thermogravimetric analysis. Going to a peak temperature higher than 170°C may be useful to see if there are any more melting points. The drop-offs in the graphs at the very end could be either complete degradation or possibly another melting point. It is interesting to note that branched polymers show lower  $T_g$  and melting points than linear polymers. According to this theory, G Series would have more branching in the polymer chains. Series A would have the least amount of branching, as it has the highest glass transition temperatures and melting points.

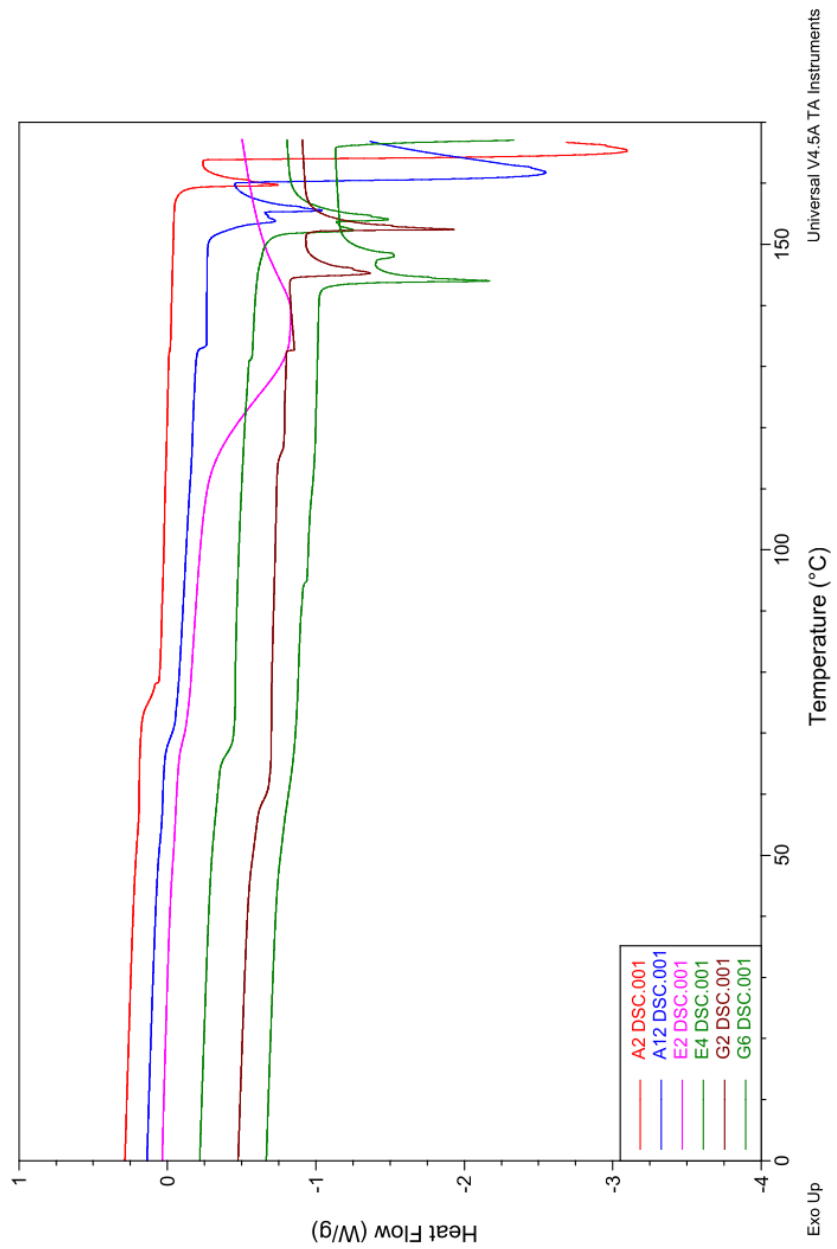


**Figure 31.** Overlay Plot of DSC thermogram for A, E and G Series.

## E. Dilute Solution Viscosity

Tables 4 and 5 (created from the viscosity tests), were used to graph Huggins and Kraemer plots. The y-intercept of the two plots gives the intrinsic viscosity, which can be used to determine the molecular weight. Shown in Figure 33 is an example of a Huggins/Kraemer plot for sample A9. A legend for all proceeding viscosity test graphs is shown in Figure 32.



Figure 32. Legend for Huggins and Kraemer Plot for calculating Intrinsic Viscosity

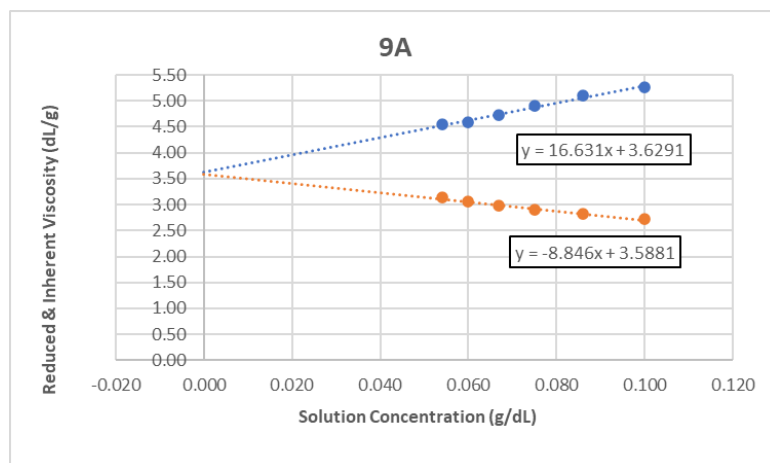
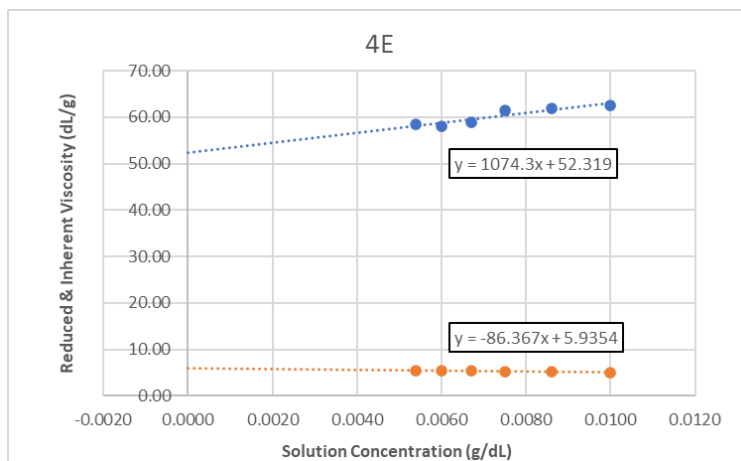
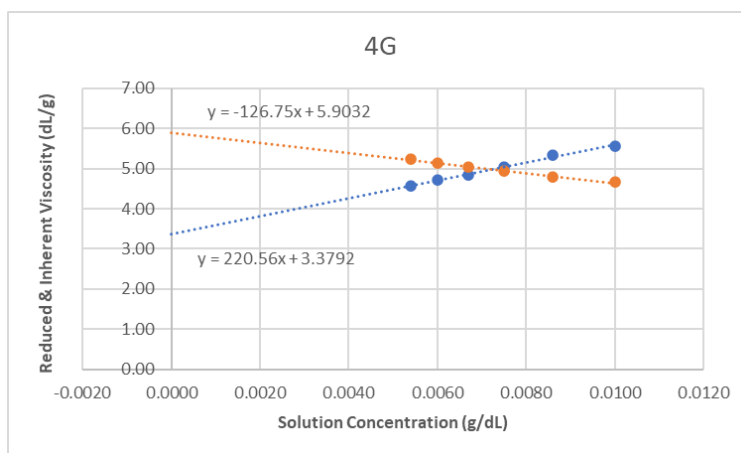


Figure 33. Huggins/Kraemer overlay graphs of Sample A9.

Although the y-intercepts of the two plots are relatively similar throughout the A series, the graphs were not as precise for the E and G series. Plots for E4 and G4 are shown below in **Figures 34 and 35**.



**Figure 34.** Huggins/Kraemer overlay graphs of Sample E4.



**Figure 35.** Huggins/Kraemer overlay graphs of Sample G4.

The Kraemer and Huggins plots in the remaining samples do not share a common y-axis. As a result the intrinsic viscosity could not be identified, and the molecular weight for these samples could not be determined. It is hypothesized that using a 0.01 g/dL solution may have introduced errors due to being at such a low concentration.

Unfortunately, at higher concentrations the solution was too viscous, so further examination is required to find the exact useful concentration. The calculated molecular weights of the A series are shown in the following **Table 11**. The equation ( $[\eta] = kM^\alpha$ ), which was obtained from previous literature, is key to determining the molecular weight. Values for  $k$  and  $\alpha$  for polyacrylamide in water are  $4.75 \times 10^{-3}$  and 0.80, respectively.<sup>30</sup>

**Table 11.** Intrinsic Viscosities and Molecular weights of A Series.

Sample	Intrinsic Viscosity ( $\eta$ ) (mL/g)	Molecular Weight (g/mol)
A3	4.46	5202.60
A5	4.17	4780.30
A9	3.61	3988.85
A10	3.50	3843.14

## CHAPTER IV: CONCLUSIONS

For this research project, three different acrylamide-based polymers were created: polyacrylamide and poly(acrylamide-co-diallyldimethylammonium chloride) via free-radical synthesis (A and E Series), and polyacrylamide via reversible addition-fragmentation chain transfer synthesis (G Series). Series A consisted of a tough pellet-like white material, while Series E was a much more brittle product and easy to crush into a powder. Series G was slightly more brittle than Series A, with a pink hue due to the RAFT agent present. Differences in structure were shown in  $^1\text{H}$  NMR and FTIR spectra, with distinct differences between the polyacrylamide and poly(acrylamide-co-diallyldimethylammonium chloride) samples, and subtler differences between the free-radical and RAFT synthesized polyacrylamides. Thermal analysis of the samples included thermogravimetric analysis and differential scanning calorimetry to show the differences in onset degradations, glass transitions, and melting point temperatures of the samples. Dilute-solution viscosity tests were used to determine the molecular weights of Series A samples but could not be used to properly determine the remaining series' molecular weights. Future work would include obtaining  $^{13}\text{C}$  NMR spectra with better noise-to-signal ratios and dilute-solution viscosity tests that could accurately provide intrinsic viscosities. This could be done by determining effective solution concentrations that are not highly viscous. A change in solvents could possibly be useful as well. Further in-depth investigation into the differences of polymer structure and molecular weights between free-radical and RAFT synthesis should also be completed. This could include adding another monomer and creating a co-monomer series via RAFT synthesis.

## REFERENCES:

1. Murugan, R., Mohan, S., & Bigotto, A. (1998). FTIR and Polarised Raman Spectra of Acrylamide and Polyacrylamide. *Journal of the Korean Physical Society*, 32(1).
2. Abdollahi, M., Ziaee, F., Alamdari, P., & Koolivand, H. (2013). A comprehensive study on the kinetics of aqueous free-radical homo- and copolymerization of acrylamide and diallyldimethylammonium chloride by online 1h-nmr spectroscopy. *Journal of Polymer Research*, 20(10). doi:10.1007/s10965-013-0239-9
3. Price, J. T., Gao, W., & Fatehi, P. (2018). Lignin-g-poly(acrylamide)-g-poly(diallyldimethyl- ammonium chloride): Synthesis, characterization and applications. *ChemistryOpen*, 7(8), 645-658. doi:10.1002/open.201800105
4. Research, T. (2018, June 29). Polyacrylamide market for water Treatment, oil & Gas, paper and other applications - global industry Analysis, SIZE, Share, growth, trends and FORECAST, 2015 - 2023: Transparency market research. Retrieved April 27, 2021, from <https://www.prnewswire.com/news-releases/polyacrylamide-market-for-water-treatment-oil--gas-paper-and-other-applications---global-industry-analysis-size-share-growth-trends-and-forecast-2015---2023-transparency-market-research-570502131.html>
5. Lin, Y., Pledger, H., Jr., & Butler, G. B. (1988). Synthesis and Characterization of Poly(diallyldimethylammonium chloride-g-acrylamide). *J. Macromol. SCI.-CHEM*, A25(8).
6. Lee, C. S., Robinson, J., & Chong, M. F. (2014). A review on application of flocculants in wastewater treatment. *Process Safety and Environmental Protection*, 92(6), 489-508. doi:10.1016/j.psep.2014.04.010
7. Zhang, Y. J., & Jia, X. (2016). Synthesis of ultra high molecular weight poly(dimethyldiallyl ammonium chloride). *Russian Journal of Applied Chemistry*, 89(2), 315-323. doi:10.1134/s10704272160020233
8. Oladoja, N. A. (2016). Advances in the quest for substitute for synthetic organic polyelectrolytes as coagulant aid in water and wastewater treatment operations. *Sustainable Chemistry and Pharmacy*, 3, (47-58). doi:10.1016/j.scp.2016.04.001
9. Rahman, M., Rana, M., Nasreen, Z., Hossain, M. M., & Sharmin, A. (2018). Treatment of Reactive Dye Containing Textile Wastewater using Microwave ASSISTED Synthesized Poly(Diallyldimethylammonium Chloride). *Journal of Bangladesh Academy of Sciences*, 41(2), 165-174. doi:10.3329/jbas.v41i2.35495
10. Sun, J., Ma, X., Li, X., Fan, J., Chen, Q., Liu, X., & Pan, J. (2018). Synthesis of a cationic polyacrylamide under uv initiation and its flocculation in estrone removal. *International Journal of Polymer Science*, 2018, 1-11. doi:10.1155/2018/8230965
11. Free radical vinyl polymerization. (n.d.). Retrieved April 11, 2021, from <https://pslc.ws/macrog/radical.htm>
12. Matyjaszewski, K. (2009). *Controlled/living radical polymerization: Progress in ATRP*. Washington, DC: American Chemical Society.
13. Matyjaszewski, K. (2000). *Controlled/living radical polymerization: Progress in ATRP, NMP, and RAFT*. Washington, D.C.: American Chemical Society.

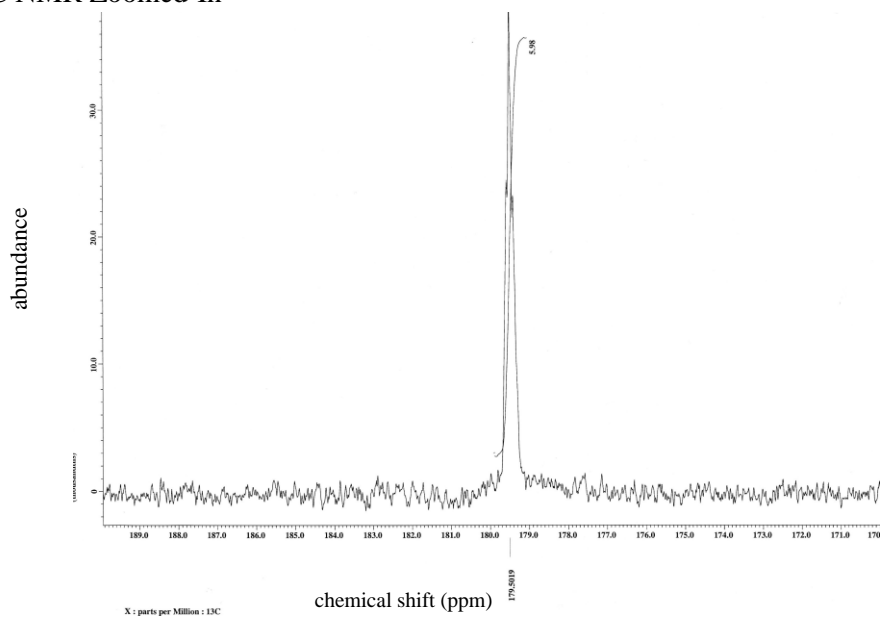
14. University, C. Features of Controlled "Living" Radical polymerizations - Matyjaszewski polymer group - Carnegie Mellon University. Retrieved April 27, 2021, from <https://www.cmu.edu/maty/crp/features.html>
15. Fishersci.com. Retrieved April 11, 2021, from <https://www.fishersci.com/shop/products/4-4-azobis-4-cyanovaleric-acid-98-cont-ca-18-water/AAH5961114>
16. Craciun, G., Ighigeanu, D., Manaila, E., & Stelescu, M. Synthesis and characterization Of Poly(Acrylamide-Co-Acrylic Acid) Flocculant obtained by electron Beam irradiation. Retrieved April 27, 2021, from [http://www.scielo.br/scielo.php?script=sci\\_arttext&pid=S1516-14392015000500984](http://www.scielo.br/scielo.php?script=sci_arttext&pid=S1516-14392015000500984)
17. G.B. Butler, Cyclopolymerization and Cyclocopolymerization, Marcel Dekker, New York, 1992
18. H. Dautzenberg, W. Jaeger, J. Kotz, B. Philipp, C. Seidel, D. Stscherbina, Polyelectrolytes-Formation, Characterization, Macromol. Sci. Chem. A21 (1984) 593. Application, Carl Hanser Verlag, Munich, 1994
19. Chen, F., Dai, D., Yang, J., Fei, Z., & Zhong, M. (2013). Controlled synthesis OF Polyelectrolytes By 4-Cyanopentanoic ACID DITHIOBENZOATE Mediated raft polymerization. *Journal of Macromolecular Science, Part A*, 50(9), 1002-1006. doi:10.1080/10601325.2013.814329
20. T.P. Le, G. Moad, E. Rizzardo, S.H. Thang , Int. Pat. WO9801478 (1998)
21. Polymer properties database. (n.d.). Retrieved April 11, 2021, from <https://polymerdatabase.com/polymer%20chemistry/RAFT.html>
22. Concepts and tools for raft polymerization. (n.d.). Retrieved April 11, 2021, from <https://www.sigmaaldrich.com/technical-documents/articles/crp-guide/concepts-and-tools-for-raft-polymerization.html>
23. S. Perrier, *Macromolecules*, 50, 19, 7433 - 7447 (2017)
24. Perrier, S. (2017). 50Th anniversary perspective: Raft polymerization—a user guide. *Macromolecules*, 50(19), 7433-7447. doi:10.1021/acs.macromol.7b00767
25. Rizzardo, E., Moad, G., & Thang, S. H. (2009). Reversible addition-fragmentation chain transfer polymerization. *Encyclopedia of Polymer Science and Technology*. doi:10.1002/0471440264.pst564
26. Cowie, J.M.G; Valeria Arrighi (2008). *Polymers: Chemistry and Physics of Modern Materials* (3rd ed.). CRC Press. ISBN 978-0-8493-9813-1.
27. Braun, D. (2009). Origins and development of initiation of free radical polymerization processes. *International Journal of Polymer Science*, 2009, 1-10. doi:10.1155/2009/893234
28. Collins, E. A., Bares, J., & Billmeyer, F. W. (1973). *Experiments in polymer science*. New York: John Wiley & Sons.
29. Al-Sabagh, A., Kandile, N., El-Ghazawy, R., Noor El-Din, M., & El-sharaky, E. (2013). Synthesis and characterization of high molecular weight hydrophobically modified polyacrylamide nanolatexes using novel nonionic polymerizable surfactants. *Egyptian Journal of Petroleum*, 22(4), 531-538. doi:10.1016/j.ejpe.2013.11.007

30. Yang, K., Chen, J., Fu, Q., Dun, X., & Yao, C. (2020). Preparation of novel amphoteric polyacrylamide and its synergistic retention with cationic polymers. *E-Polymers*, 20(1), 162-170. doi:10.1515/epoly-2020-0026

## APPENDIX A: NMR Spectroscopy Data

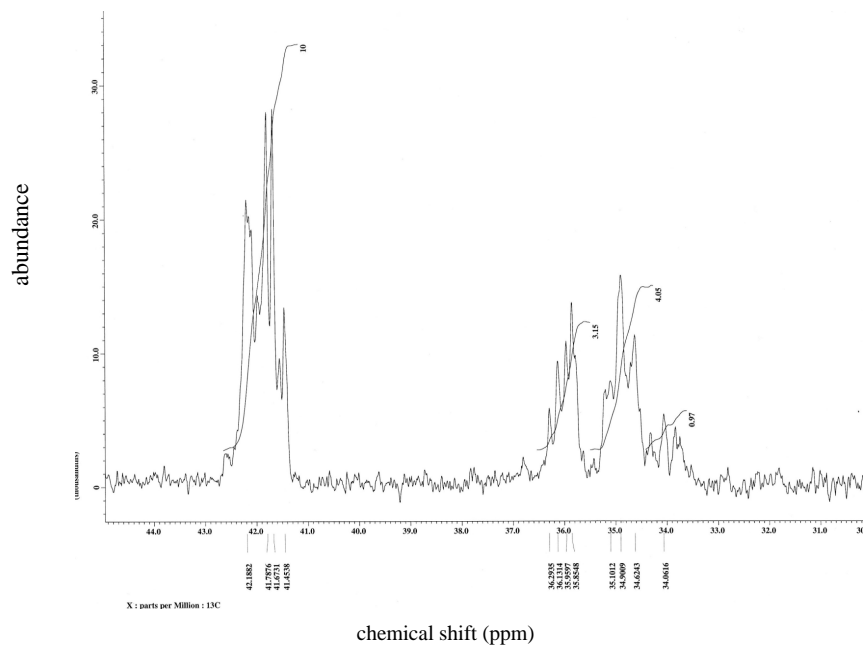
### 1. Polyacrylamide: Sample A8

$^{13}\text{C}$  NMR Zoomed-In



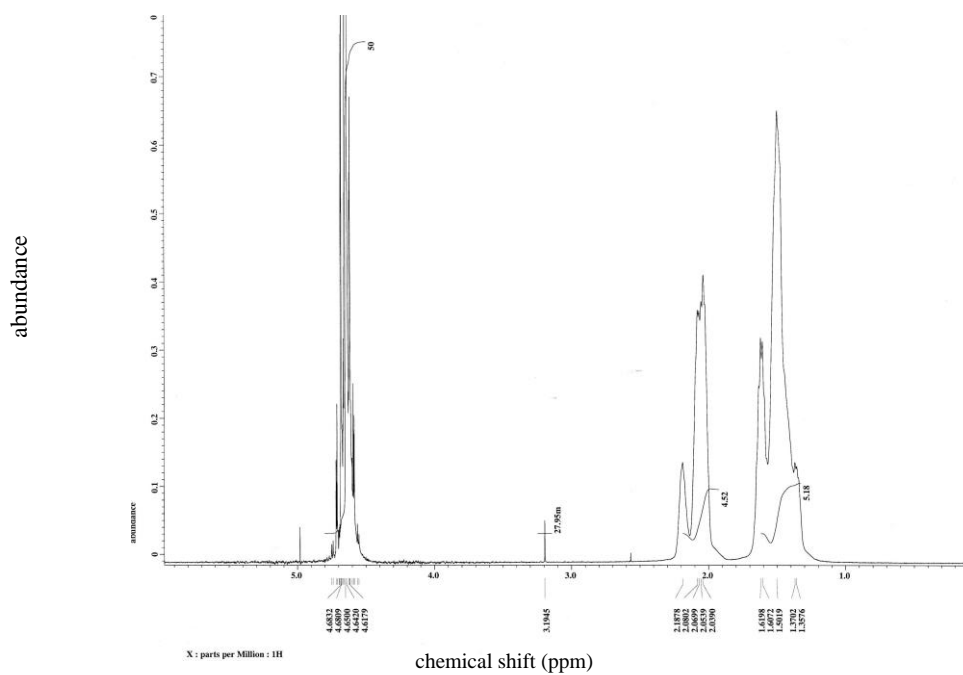
### 2. Polyacrylamide: Sample A8

$^{13}\text{C}$  NMR Zoomed-In



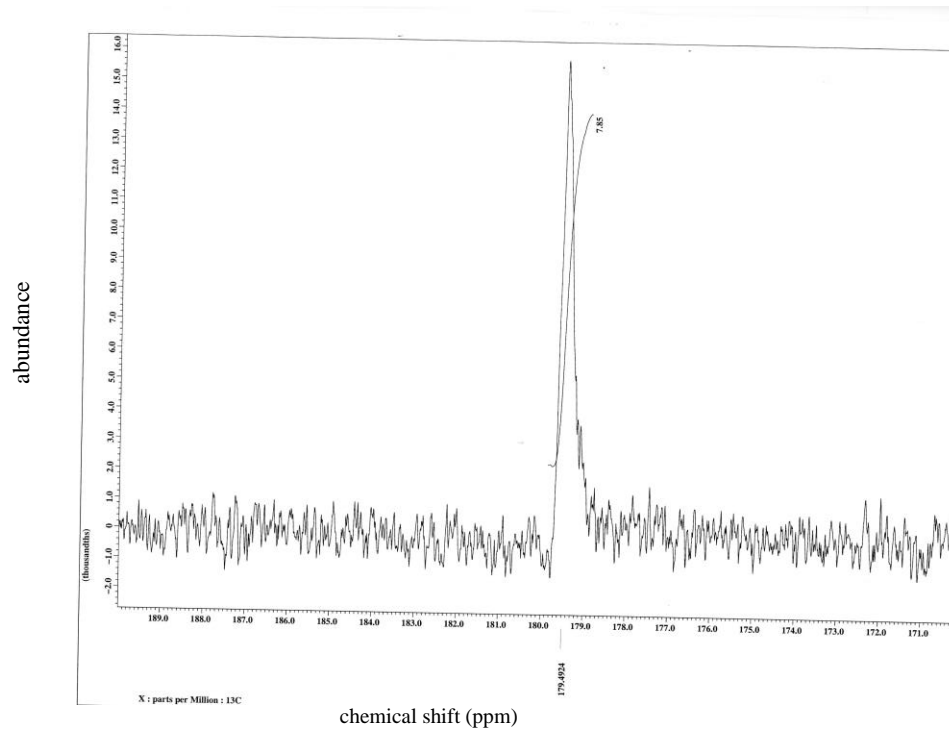
### 3. Polyacrylamide: Sample A8

### <sup>1</sup>H NMR Zoomed-In



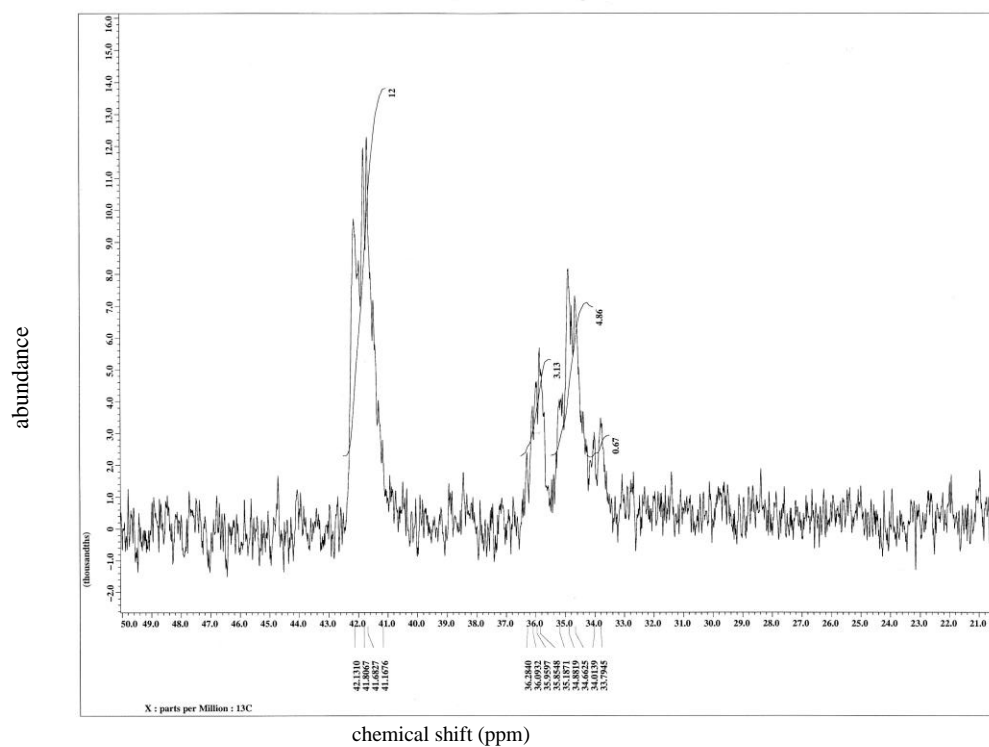
### 4. Poly(acrylamide-co-diallyldimethylammonium chloride): Sample E4

#### <sup>13</sup>C NMR Zoomed-In



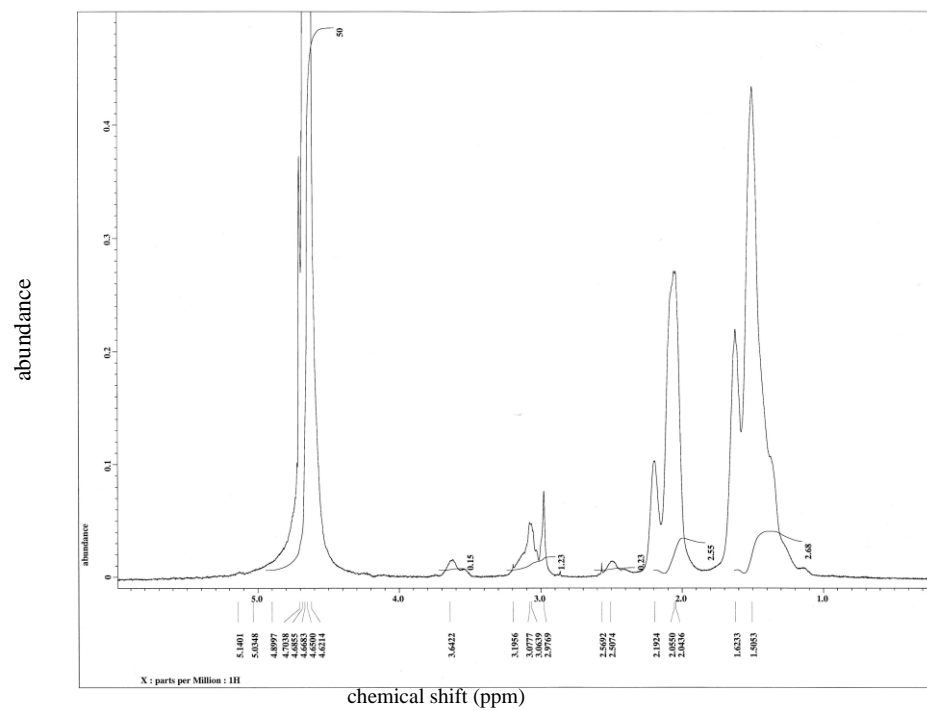
### 5. Poly(acrylamide-co-diallyldimethylammonium chloride): Sample E4

### $^{13}\text{C}$ NMR Zoomed-In



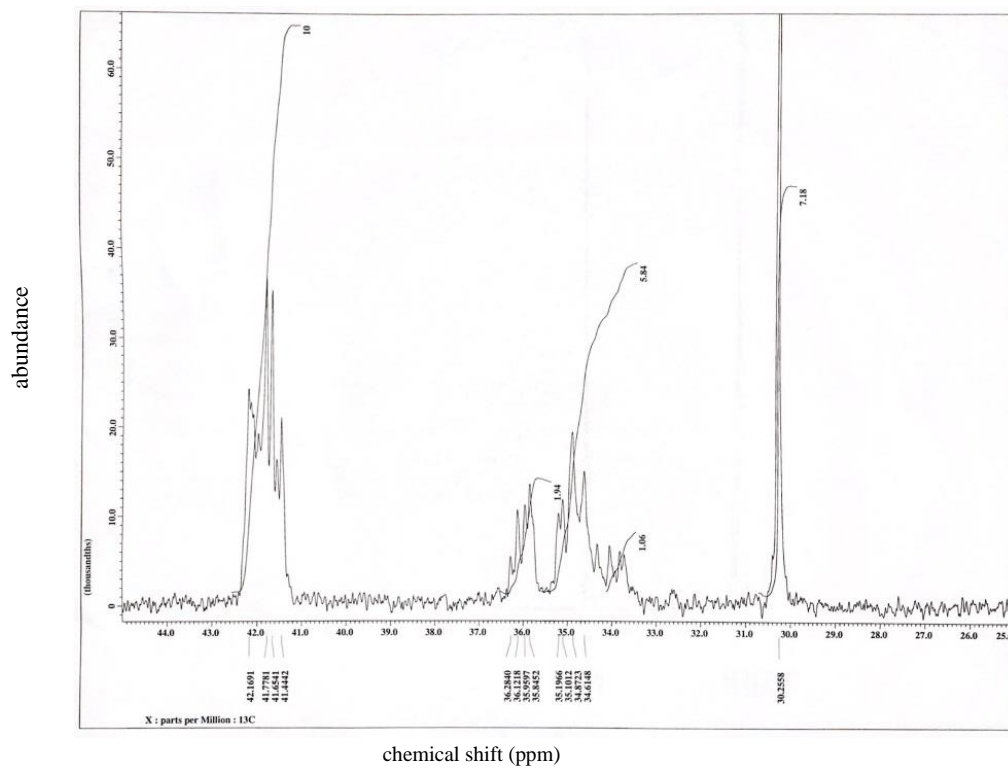
### 6. Poly(acrylamide-co-diallyldimethylammonium chloride): Sample E4

#### $^1\text{H}$ NMR Zoomed-In



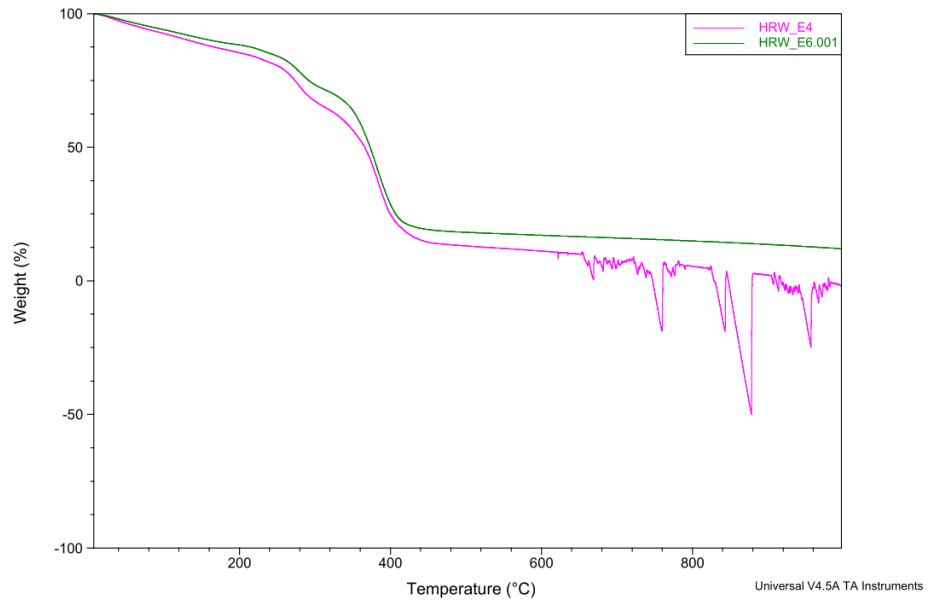
### 7. Polyacrylamide: Sample G4

$^{13}\text{C}$  NMR Zoomed-IN

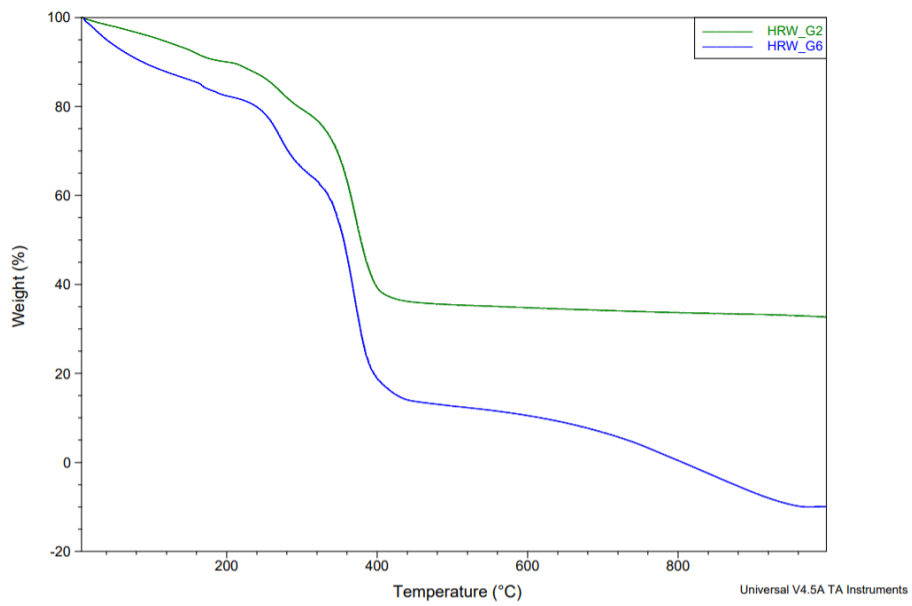


## APPENDIX B: Thermal Analysis Data

### 1. TGA Overlay plot of Samples E4 and E6

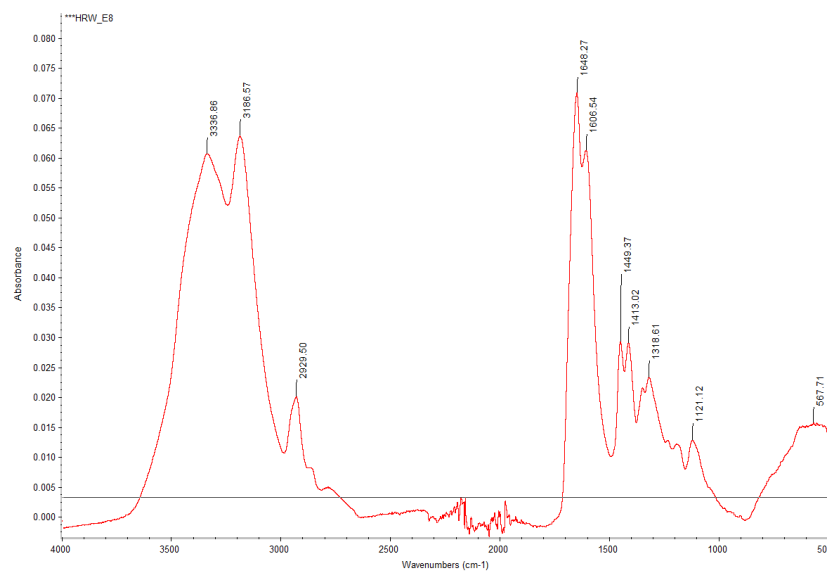


### 2. TGA Overlay plot of Samples G2 and G4



## APPENDIX C: FTIR Analysis Data

### 1. FTIR plots specific peak assignments: Sample E8



### 2. FTIR plots specific peak assignments: Sample G4

